Iranian Journal of Fuzzy Systems

Volume 22, Number 3, (2025), pp. 55-86

Original paper

University of Sistan and Baluchestan

Molecular fuzzy least squares optimization-based decision making with entropy expert weighting for transparent solar panel installation investments

G. Kou [1], H. Dinçer [2], S. Yüksel [3], C. Demir [4] and S. Eti [5]

[1] *School of Business Administration, Faculty of Business Administration, Southwestern University of Finance and Economics, Chengdu 611130, China*

[1] *School of Digital Media Engineering and Humanities, Hunan University of Technology and Business, Changsha 410205, China*

[2,3] *School of Business, Istanbul Medipol University, Istanbul, Turkey*

[2,3] *Department of Economics and Management, Khazar University, Baku, Azerbaijan*

[2,3] *Clinic of Economics, Azerbaijan State University of Economics (UNEC), Baku, Azerbaijan*

[4] *School of Business, Istanbul Medipol University, Istanbul, Turkey*

[5] *IMU Vocational School, Istanbul Medipol University, Istanbul, Turkey*

kougang@swufe.edu.cn, hdincer@medipol.edu.tr,serhatyuksel@medipol.edu.tr, ceren.demir1@medipol.edu.tr, seti@medipol.edu.tr

Abstract

The performance of transparent solar panel projects is affected by both technological and environmental and economic factors. However, the most important items should be identified for the efficient use of limited resources and effective risk management. There are few studies in the literature determining these factors. Because of this situation, businesses cannot direct their resources correctly and cannot create an effective strategy. A molecular fuzzy decision-making system is created to determine the most successful alternative investment policies for these projects to satisfy this gap in the literature. Various techniques are integrated in this model to reach the most effective solutions, such as molecular fuzzy sets to handle uncertainties, q-learning algorithm to weight experts, least square optimization (LSO) to calculate criteria weights and multi-objective particle swarm optimization (MOPSO) to rank investment strategies. The main contribution of this study is proposing an innovative molecular fuzzy decision-making model that manages uncertainties more effectively to select the most appropriate investment strategies for transparent solar panel investments. Considering molecular fuzzy sets allows for more accurate modelling of uncertainties and subjective evaluations. The results show that the most critical investment criterion for transparent solar panel investments is the regional solar radiation level.

Keywords: Molecular fuzzy sets, least square optimization, q-learning, solar panels, energy economics.

1 Introduction

Transparent solar panel installation investments are new generation solar energy projects carried out to make energy production more aesthetic. These panels can be integrated into glass surfaces. With the help of this issue, some of the light obtained can pass through while some of it can produce electricity. These projects have some advantages compared to their counterparts. Traditional solar panels can only be installed on roofs. In contrast, transparent solar panels can be integrated into many surfaces such as building windows. This situation contributes to achieving energy efficiency, especially in high-rise buildings (Fahoum and Sitbon, 2025). Another advantage of these panels is that they support the reduction of fossil fuel use. Owing to this situation, the carbon emission problem can be significantly reduced. There are variables that need to be taken into consideration to increase the performance of transparent solar panel projects. Conversion efficiency is an important factor in this process. The capacity of the panel to convert incoming light into

Corresponding Author: S. Yüksel

Received: June 2025; Accepted: Invited paper.

https://doi.org/10.22111/ijfs.2025.9246

electricity directly affects energy production. The durability of the materials used also plays a very important role in this process. The size of the surface where the panel is placed also affects performance (Habchi et al., 2025). It is possible to increase energy production in panels where more sunlight is received. The investment return period also shows how long the project will take to turn a profit. Projects that are financially successful are also more likely to attract the attention of investors.

The performance of these projects is affected by both technological and environmental and economic factors. To develop an effective strategy, it is necessary to determine the most important of these factors. This is primarily required for the efficient use of resources. Each project is carried out with a limited budget, time and human resources. Focusing on the most effective variables supports the increase of efficiency in this process. Determining these factors is also important for further increasing the performance of these projects. It is not a correct practice to approach all factors equally (Luo et al., 2025). Instead, creating strategies focused on high-impact factors produces stronger results. Not identifying these factors leads to investments in areas with low impact on performance. Similarly, not knowing the impact of each variable increases unforeseen problems. Therefore, determining the variables with the highest importance is indispensable for optimizing the project. There are few studies in the literature determining these factors. Therefore, it is not clear which factors businesses should prioritize and develop strategies (Liu et al., 2025). This situation is considered a deficiency in the literature. Many studies in the literature list technological, environmental or economic variables. However, it has not been clarified which of these variables are more critical. Due to this situation, businesses cannot direct their resources correctly and cannot create an effective strategy.

To address this research gap in the literature, a molecular fuzzy decision-making system is generated to determine the most successful alternative investment policies for transparent solar panel installations. This proposed model can be helpful to implement prior strategies to improve the performance of these projects. Various techniques are integrated in this model to reach the most effective solutions. In this scope, q-learning algorithm based on the entropy game is applied to compute the weights of the experts. Next, investment criteria are weighted with least square optimization (LSO). Moreover, alternative investment policies are ranked with multi-objective particle swarm optimization (MOPSO). On the other side, molecular fuzzy sets are also implemented to handle uncertainties in the analysis process more successfully. There are many studies in the existing literature that list technological, environmental and economic factors. However, the importance levels among these factors have not been clearly stated. Due to this deficiency, businesses do not know which factors they should prioritize. Therefore, the scarcity of studies on determining the variables with the highest importance level is one of the main motivations of this study. On the other hand, decision-making models can be used in the literature to determine the priority factors. Comprehensive models that take innovative techniques into account are needed to obtain more reliable and realistic results in decision-making processes. Furthermore, fuzzy sets and other techniques used in the model should also be suitable for the research topic. The optimization capability of the models in the literature is generally limited. However, in the real world, investment decisions usually require evaluating multiple goals, conflicting criteria and dynamic expert opinions together. It is seen that a new decision-making model is needed in this field. This deficiency also emerges as another motivation for this study. In summary, this study aims to answer the following research questions.

(1) Among technological, environmental and economic factors, which ones affect the performance of transparent solar panel investments the most?

(2) In which aspects, does the newly developed molecular fuzzy decision-making model produce more successful results compared to existing decision-making approaches?

(3) How do the investment strategies suggested by the new model improve the performance of transparent solar panel projects?

(4) Which alternative strategies have a higher potential to increase performance in transparent solar panel investments?

This study contributes to the literature by proposing an innovative molecular fuzzy decision-making model that manages uncertainties more effectively to select the most appropriate investment strategies for transparent solar panel investments. There are some criticisms towards decision-making models in the literature. Traditional decision-making methods may not be able to manage uncertainty effectively enough. Moreover, old models may be inadequate in evaluating multiple objectives and conflicting criteria. In addition, in classical models, the reliability and weighting of expert opinions are usually inadequate. This new decision-making model can overcome the basic deficiencies of old models in the literature. The basic advantages of this proposed model are given below.

(1) There are some advantages of preferring molecular fuzzy sets in this proposed model. Molecular fuzzy sets are obtained by integrating molecular geometry with fuzzy logic. Molecular fuzzy sets allow for more accurate modelling of uncertainties and subjective evaluations. This provides more reliable and precise results in decision-making processes. Molecular geometry helps to express information with multi-dimensional and very complex structures. Thus, a more effective comparison can be made between various aspects of each alternative in multi-criteria decision-making systems.

Traditional fuzzy sets usually define uncertainty only through membership functions. This may be incomplete in dynamic and multi-dimensional data. Molecular fuzzy sets provide richer and more accurate information transfer by integrating molecular geometry. Interval type-2 fuzzy sets may be less efficient in terms of computational complexity and model applicability. Molecular fuzzy sets, on the other hand, provide more effective calculation opportunities for complex processes by taking inspiration from different geometric shapes.

(2) Preferring LSO in calculating the criterion weights in your proposed model increases the quality of the model. LSO minimizes the squares of the differences between the actual values and the model estimates in determining the criterion weights. In this way, the deviations that cause errors can be reduced. This allows for more accurate criterion weights to be obtained. Another advantage of this application is that it can be easily integrated with different fuzzy set types. Techniques such as decision-making trial and evaluation laboratory (DEMATEL) and criteria importance through intercriteria correlation (CRITIC) are also taken into consideration in criterion weighting. However, optimization is not performed in these approaches. Instead, the relationships are analyzed qualitatively. Similarly, these techniques may not produce precise results when there are many criteria. LSO, on the other hand, shows high performance especially in complex systems with many criteria.

(3) In the proposed model, determining expert weights with the q-learning algorithm provides a meaningful and innovative contribution to the literature. In most classical decision-making models, the opinions of experts are considered equally important. On the other hand, experts usually have different knowledge levels. Therefore, giving equal weight to all experts may reduce accuracy and reliability in the decision-making process. The q-learning algorithm dynamically updates the weights of each expert according to their contribution level to the decision process. Experts who make the most accurate predictions gain higher importance. This method increases the accuracy and reliability of decision support systems.

The organization of the manuscript is demonstrated as follows. The missing gap in the literature about this subject is underlined in the second section. A novel model is proposed in the third section to address this missing part. The main results are explained in the following section. The fifth section focuses on the discussion with similar studies in the literature. The final section identifies the main concluding remarks.

2 Literature review

Studies have reported that energy consumption can be met sustainably by determining a sufficiently large solar photovoltaic system (Umair et al., 2024a). Having a sustainable energy source also means a stable power source (Wang et al., 2024). However, applying in practice of this work, financial assistance programs and financial regulations such as various tax incentives and feed-in tariffs for solar photovoltaic installations are critical (Wang et al. 2024a). The study examining the energy autonomy (the ratio of on-site energy production to total energy demand) of greenhouses equipped with semi-transparent photovoltaic (STPV) systems with Battery Energy Storage System (BESS) highlighted the relationship between prices and risks (Gholami et al., 2025). The use of BESS can provide a more predictable energy cost structure and reduce financial risks associated with energy price volatility (Hussain et al., 2024a, 2024b). Another study with a risk assessment to evaluate economic viability and potential barriers to residential PV solar adoption showed that competitive payback periods and favourable returns on investment can offer cost-effective solutions (Shand et al., 2025). However, it is also important to note that there will be differences in risk perception between regulators and investors regarding the impact of risks (Aziz et al., 2025).

According to Abu Qadourah and Alnusairat (2024), it is necessary to examine PV installations by considering both their functionality and aesthetics. In this context, they investigated how PV systems affect the perception of PV installations by evaluating the aesthetic dimensions. In the development of solar energy systems, there is a growing attention on combining innovative design with aesthetic integration into urban environments (Bonomo and Frontini, 2024). One such approach explores the use of solar cells to form both artistic and functional structures on spherical and hemispherical surfaces. While spherical designs are often present superior aesthetics for their visual appeal, hemispherical configurations tend to offer greater efficiency (Almadhhachi et al., 2024). Besides the perceived benefits of solar energy, the aesthetics of PV installations and the equitable distribution of these benefits among different social groups influence public acceptance (Gholami, 2024). Therefore, new systems that aim to provide and distribute efficiency more effectively have inevitably become a part of architectural design. Building-integrated photovoltaics (BIPV) concordantly act as an important component of architectural design. In this context, parameters such as shape, size and colour become important. (Borja Block et al., 2024). On the other hand, BIPV is conducting life cycle cost analyses for the economic viability with its facilities (Bonomo et al., 2024;). Therefore, BIPV provides buildings with renewable energy while also improving their appearance. By incorporating photovoltaic modules into building facades, roofs, or windows, it allows buildings to effectively capture sunlight and transform it into clean energy. On the other

hand, they often face high electricity costs due to substantial energy consumption from industrial processes (Zhang et al., 2025).

The important role of distributed rooftop solar panels in the carbon neutralization process has made research into the investment potential in this area. These investments can increase the expected profits of public service companies and achieve social goals by offsetting the welfare transfer effect (Chen et al., 2024). The economic aspects of solar tracking systems (STS), which increase the efficiency of photovoltaic modules by dynamically adjusting them, need to be examined. According to Kazem et al. (2024), This system has a clear benefit in terms of renewable energy use and minimization of greenhouse gas emissions. On the other hand, high implementation and maintenance costs create fluctuations in their efficiency. In addition, the lack of standardized solutions and qualified personnel may have an impact on investment decisions (Wu et al., 2024). Having said that, there are also studies explaining that these systems will increase efficiency and achieve savings with dual-axis tracking and one-axis tracking for the efficient use of solar energy (Forhad et al., 2024). Other results indicate that, on average, renewable energy systems provide more net useful energy per unit of final energy invested compared to fossil fuels (Aramendia et al., 2024). Additionally, cost-benefit analysis of STS shows that solar tracker-based HES as a cost-effective option for rural energy needs (Kumba et al., 2024). The importance of using affordable energy storage batteries to encourage the use of solar energy systems in developing economies with limited financial resources has also been highlighted in another study (Tham et al., 2025).

One of the most important criteria for the efficiency of solar panels is the region where the installation is made. The amount of solar irradiation is directly related to the climate of the region. Solar irradiation refers to the quantity of energy that reaches a given area over a specified period, and expressed as (kWh/m^2), so it inevitably affects a region's capacity to generate solar energy (Fragkos et al., 2025). As a result, in areas with high solar irradiation, the return on investment (ROI) period can be shorter (Zhang, 2025). More energy is produced in these areas, and more savings can be achieved. To make a real performance assessment, solar irradiation data that determines the size and capacity of a PV system must be analyzed (Qamili and Kapia, 2024). The findings of another study indicate that a one-axis tracking system is the most advantageous choice for maximizing radiation collection on behalf of the cost–benefit ratio (Li et al., 2025). It is strongly recommended to implement a one-axis tracking system in solar installations across the Mediterranean region due to the high costs associated with the installation and maintenance of two-axis tracking systems (Akgul et al., 2024). Although solar panels are powered by the sun, surprisingly, their efficiency performance can deteriorate as temperatures rise. Minazhova et al. (2025) reporting that PV panels tend to experience significant heating during the summer months, leading to a 5-10% decrease in efficiency and deterioration of the panels. In this context, it becomes necessary to also implement a cooling system for PV panels. Therefore, considering the efficiency that will vary from time to time, a long-term and strong investment analysis is required in this area. It's noteworthy that supportive measures such as subsidies, grants can bring solar energy to a financially optimistic point (Andrade-Arias et al., 2025).

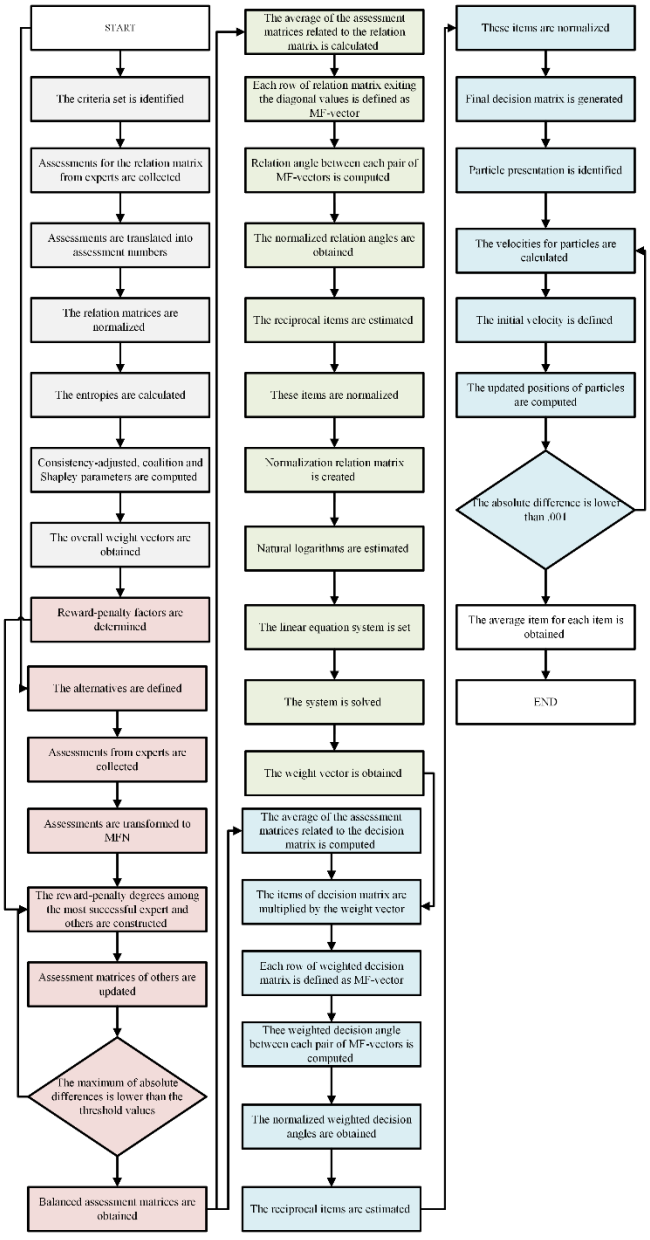
The subject of transparent solar panels is among the topics that have gained considerable importance in the literature in recent years. Studies address the potential that transparent solar panels can create in renewable energy. When considered from this perspective, various criteria come to the fore for research. On the other hand, there are a limited number of studies that determine which variables are more important in these studies. This situation can create uncertainty for investment decisions. Determining the best factors is very important to encourage businesses to make the right strategic investment decisions. Businesses have limited financial resources. Therefore, studies that will allow businesses to use their limited financial resources more efficiently will add diversity to the literature. The lack of studies that determine the most critical factors indicates an important deficiency in the solar panel literature. To eliminate this deficiency, new studies that include analyses on the determined criteria are needed.

3 Methodology

In this paper, a molecular fuzzy decision-making system is generated to determine the most successful alternative investment policies for transparent solar panel installations in buildings. In this generated system, investment criteria are weighted with LSO, while alternative investment policies are ranked with MOPSO. In this process, molecular fuzzy sets are used based on the linguistic scale. Thus, uncertainty is analysed and the analysis findings become more realistic and accurate. In addition, due to the different experiences of the experts, assessment matrices need to be balanced. For this purpose, the Q-learning algorithm is applied. The expert weights for the reward-penalty parameters in the Q-learning algorithm are calculated based on the Entropy game. The operation of the system is visualized in Figure 1.

Molecular fuzzy sets $\mathcal{X}$ in a universe of discourse $\mathfrak{S}$ are processed to define the relationships in a multidimensional scape. Let $\S = (\mathfrak{M},\ \mathfrak{N},\ \mathfrak{H}\ )$, then this set is an object having the form in Equation (1).

Figure 1: The Operation of The System



$$\mathfrak{M}_{\mathcal{X}}(\S)+\mathfrak{N}_{\mathcal{X}}(\S)+\mathfrak{H}_{\mathcal{X}}(\S)=1. \tag{1}$$

According to molecular geometry analysis, the membership of the MFF is computed as normalized angles via Equation (2).

$$\mathfrak{M}_{\mathcal{X}}(\S)=\{(\wp_{\S})=1-\frac{\wp_{\S}}{\wp_{\max}}. \tag{2}$$

Wherein $\wp_{\S}$ presents the normalized angle of the $\mathfrak{M}$ for $\S$. $\{(\wp_{\S})$ is the monotonically decreasing function. The value of this function is between 0 and 1. $\wp_{\max}$ means the maximum normalized angle in the matrix or the angle of molecular geometry shapes such as linear, trigonal planar, tetrahedral, trigonal bipyramidal, and octahedral. This shapes' radians (degrees) are π (180°), $\frac{\pi}{3}$(120°), 1.91 (109.5°), 1.83 (105°) and $\frac{\pi}{2}$ (90°), respectively. The non-membership is identified by Equation (3).

$$\mathfrak{N}_{\mathcal{X}}(\S)=\frac{\wp_{\S}}{\wp_{\max}}. \tag{3}$$

Similarly, the hesitant is computed with Equation (4).

$$\mathfrak{H}_{\mathcal{X}}(\S)=1-\left(\left(1-\frac{\wp_{\S}}{\wp_{\max}}\right)+\frac{\wp_{\S}}{\wp_{\max}}\right). \tag{4}$$

Let $\mathcal{Z}$ and $\mathcal{Y}$ be two MFSs, then subset of $\mathcal{Y}$ is defined for $\mathcal{Z}$ by Equation (5).

$$\mathcal{Z}\subseteq\mathcal{Y}\leftrightarrow\mathfrak{M}_{\mathcal{Z}}(\S)\leq\mathfrak{M}_{\mathcal{Y}}(\S)\ \&\ \mathfrak{N}_{\mathcal{Z}}(\S)\leq\mathfrak{N}_{\mathcal{Y}}(\S)\ \&\ \mathfrak{H}_{\mathcal{Z}}(\S)\geq\mathfrak{H}_{\mathcal{Y}}(\S);\ \forall\S\in\mathcal{X}. \tag{5}$$

The equality condition is given in Equation (6).

$$\mathcal{Z}=\mathcal{Y}\leftrightarrow\mathcal{Z}\subseteq\mathcal{Y}\ \&\ \mathcal{Y}\subseteq\mathcal{Z}. \tag{6}$$

The union operator is defined in Equation (7).

$$\mathcal{Z}\cup\mathcal{Y}=\{(\S,\max(\mathfrak{M}_{\mathcal{Z}}(\S),\mathfrak{M}_{\mathcal{Y}}(\S)),\min(\mathfrak{N}_{\mathcal{Z}}(\S),\mathfrak{N}_{\mathcal{Y}}(\S)),\min(\mathfrak{H}_{\mathcal{Z}}(\S),\mathfrak{H}_{\mathcal{Y}}(\S)))\mid\S\in\mathcal{X}\}. \tag{7}$$

The intersection operator is identified in Equation (8).

$$\mathcal{Z}\cap\mathcal{Y}=\{(\S,\min(\mathfrak{M}_{\mathcal{Z}}(\S),\mathfrak{M}_{\mathcal{Y}}(\S)),\max(\mathfrak{N}_{\mathcal{Z}}(\S),\mathfrak{N}_{\mathcal{Y}}(\S)),\max(\mathfrak{H}_{\mathcal{Z}}(\S),\mathfrak{H}_{\mathcal{Y}}(\S)))\mid\S\in\mathcal{X}\}. \tag{8}$$

The multiplication operator is determined in Equation (9).

$$\mathcal{Z}\cdot\mathcal{Y}=\{(\S,\mathfrak{M}_{\mathcal{Z}}(\S)\cdot\mathfrak{M}_{\mathcal{Y}}(\S),\mathfrak{N}_{\mathcal{Z}}(\S)\cdot\mathfrak{N}_{\mathcal{Y}}(\S),\mathfrak{H}_{\mathcal{Z}}(\S)\cdot\mathfrak{H}_{\mathcal{Y}}(\S))\mid\S\in\mathcal{X}\}. \tag{9}$$

The scalar multiplication operator is estimated in Equation (10). $\lambda>0$

$$\lambda\mathcal{Y}=\{(\S,\min(\lambda\cdot\mathfrak{M}_{\mathcal{Y}}(\S),1),\max(1-\lambda(1-\mathfrak{N}_{\mathcal{Y}}(\S)),0),\max(1-\lambda(1-\mathfrak{H}_{\mathcal{Y}}(\S)),0))\mid\S\in\mathcal{X}\}. \tag{10}$$

The exponentiation operator is shown in Equation (11).

$$\mathcal{Y}^{\lambda}=\{(\S,(\mathfrak{M}_{\mathcal{Y}}(\S))^{\lambda},1-(1-\mathfrak{N}_{\mathcal{Y}}(\S))^{\lambda},1-(1-\mathfrak{H}_{\mathcal{Y}}(\S))^{\lambda})\mid\S\in\mathcal{X}\}. \tag{11}$$

The complement of $\mathcal{Y}$ is given in Equation (12).

$$\mathcal{Y}^{c}=\{(\S,\mathfrak{N}_{\mathcal{Y}}(\S),\mathfrak{H}_{\mathcal{Y}}(\S),\mathfrak{M}_{\mathcal{Y}}(\S))\mid\S\in\mathcal{X}\}. \tag{12}$$

3.1 Entropy game-based Q-learning

Due to the differences in the professional characteristics of the experts, there may be an imbalance in assessments of experts. This imbalance is overcome by the Q-learning algorithm. The Q-learning algorithm includes reward-penalty factors. These factors are determined from the weights of the experts for MCDM. In calculating these weights, the objective method Entropy Game is integrated into the algorithm. The steps of the updated algorithm are introduced below (Dinçer et al., 2025).

At the beginning of the updated algorithm, assessments for the relation matrix from experts are collected and these assessments are translated into assessment numbers. A relation matrix $\left(\mathcal{QR}_{ij}^{t}\right)$ is established for each expert. Next, the relation matrices are normalized with Equation (13).

$$\mathcal{QR}_{ij}^{t}=\frac{\dashv\backslash_{ij}^{t}}{\sum_{i=1}^{n-1}\dashv\backslash_{ij}^{t}}. \tag{13}$$

Wherein n is the number of criteria. $\dashv\backslash_{ij}^{t}$ presents the assessment number in relation matrix for t^{th} expert. Then, the entropies of $\mathcal{QR}_{j}$ are calculated for experts with the help of Equation (14).

$$\mathcal{E}_{j}^{t}=-\frac{1}{\ln(n-1)}\sum_{i=1}^{n-1}\mathcal{QR}_{ij}^{t}\ln\left(\mathcal{QR}_{ij}^{t}\right). \tag{14}$$

Afterwards, consistency-adjusted, coalition and Shapley parameters are computed using Equations (15)-(17), respectively.

$$\rfloor\dashv^{t}=1-\frac{\sum_{j=1}^{n}\mathcal{E}_{j}^{t}}{n}. \tag{15}$$

$$\rfloor\sqsubseteq(\mathcal{S})=\sum_{t\in\mathcal{S}}\rfloor\dashv^{t}\sum_{i=1}^{n-1}\sum_{j=1}^{n-1}\mathcal{QR}_{ij}^{t}. \tag{16}$$

$$\int\sqsubseteq^{t}=\sum_{\mathcal{S}\subseteq\mathcal{N}\backslash\{t\}}\frac{|\mathcal{S}|!\left(|\mathcal{N}|-|\mathcal{S}|-1\right)!}{|\mathcal{N}|!}\rfloor\sqsubseteq(\mathcal{S}\cup\{t\})-\rfloor\sqsubseteq(\mathcal{S}). \tag{17}$$

Wherein $\mathcal{N}$ is the experts' set. $|\mathcal{S}|$ is the number of objects in subset $\mathcal{S}$. Later, the overall weight vectors are obtained by Equation (18).

$$\wr^{t}=\frac{\int\sqsubseteq^{t}}{\sum_{t=1}^{|\mathcal{N}|}\int\sqsubseteq^{t}}. \tag{18}$$

The penalty factor for Q-learning algorithm is equal to the maximum of $\wr$. The reward factors are equal to the other $\wr$ values. After determining the factors, the assessments are collected and transformed to MFN. The reward-penalty degrees among the most successful expert and others are constructed with Equations (19) and (20).

$$\mathcal{RD}_{s,a}=\wr^{t}\left(\mathcal{Q}_{s,a}^{mse}-\mathcal{Q}_{s,a}^{oe}\right). \tag{19}$$

$$\mathcal{PD}_{s,a}=\max\left(\wr^{t}\right)\left(\mathcal{Q}_{s,a}^{oe}-\mathcal{Q}_{s,a}^{mse}\right). \tag{20}$$

Wherein $\mathcal{Q}_{s,a}^{mse}$ is assessment matrix of the most successful expert and $\mathcal{Q}_{s,a}^{oe}$ is the assessment matrices for others. Using reward-penalty degrees, assessment matrices of others are updated according to the most successful expert using Equation (9).

$$\mathcal{Q}_{s,a}^{\sqcap} = \mathcal{Q}_{s,a}^{mse} + \{ \left(\mathcal{RD}_{s,a} - \mathcal{PD}_{s,a} \right). \tag{21}$$

Wherein { refers to learning rate of algorithm. This updating is continuous until the maximum of absolute differences between the initial and updated assessment matrices is lower than the threshold values. In other word, Equations (22) and (23) is tested.

$$\Delta_{s,a} = \mid \mathcal{Q}_{s,a}^{\sqcap} - \mathcal{Q}_{s,a} \mid . \tag{22}$$

$$\Delta_{\max} = \max_{s,a} \{ \Delta_{s,a} \}. \tag{23}$$

Until the condition is met, the reward-penalty degrees are recalculated, and the assessment matrices are updated. When the condition is met, balanced assessment matrices are obtained.

3.2 MF-LSO-based MOPSO

LSO is the original method that constructs the criteria weight vector by minimizing the sum of squared errors among the elements of the relation matrix. This method establishes a linear equation system and obtains the criterion weight vector by solving this system. MOPSO is a technique established to solve complex problems. This technique reveals the relationship between alternatives and ranks the alternatives. In the process of this technique, it produces pareto-optimal solutions and then produces balanced results. The process of combining these two techniques is shown below (Budhiraja et al., 2025).

At the beginning of the combining these two techniques, the average of the assessment matrices related to the relation matrix is calculated by Equations (24) and (25).

$$\dashv \sqsubseteq_{ij} = \left(\frac{1}{|\mathcal{N}|} \sum_{t=1}^{|\mathcal{N}|} \mathfrak{M}_{ij}^{t}, \frac{1}{|\mathcal{N}|} \sum_{t=1}^{|\mathcal{N}|} \mathfrak{N}_{ij}^{t}, \frac{1}{|\mathcal{N}|} \sum_{t=1}^{|\mathcal{N}|} \mathfrak{H}_{ij}^{t} \right). \tag{24}$$

$$\mathcal{AV} = [\dashv \sqsubseteq_{ij}]_{n \times n}. \tag{25}$$

Wherein $\mathfrak{M}$, $\mathfrak{N}$ and $\mathfrak{H}$ are the degrees of membership (MS), non-MS and hesitancy, respectively and the sum of degrees equals to 1. Next, each row of relation matrix exiting the diagonal values is defined as MF-vector as Equation (26). Because these values are empty.

$$\mathfrak{w}_i = \left[\left(\mathfrak{M}_{i1}, \mathfrak{N}_{i1}, \mathfrak{H}_{i1} \right), \left(\mathfrak{M}_{i2}, \mathfrak{N}_{i2}, \mathfrak{H}_{i2} \right), \ldots, \left(\mathfrak{M}_{in-1}, \mathfrak{N}_{in-1}, \mathfrak{H}_{in-1} \right) \right]. \tag{26}$$

Later, the relation angle between each pair of MF-vectors is computed using Equations (27) – (29).

$$\left(\mathfrak{w}_i \mathfrak{w}_j \right) = \sum_{l=1}^{n-1} \left(\mathfrak{M}_{i,l} \mathfrak{M}_{j,l} + \mathfrak{N}_{i,l} \mathfrak{N}_{j,l} + \mathfrak{H}_{i,l} \mathfrak{H}_{j,l} \right). \tag{27}$$

$$\cos \wp_{\mathfrak{w}_i, \mathfrak{w}_j} = \frac{\left(\mathfrak{w}_i \mathfrak{w}_j \right)}{\left(\sum_{l=1}^{n-1} \left(\mathfrak{M}_{i,l}^2 + \mathfrak{N}_{i,l}^2 + \mathfrak{H}_{i,l}^2 \right) \right) \left(\sum_{l=1}^{n-1} \left(\mathfrak{M}_{j,l}^2 + \mathfrak{N}_{j,l}^2 + \mathfrak{H}_{j,l}^2 \right) \right)}. \tag{28}$$

$$\wp_{\mathfrak{w}_i, \mathfrak{w}_j} = \cos^{-1} \left(\cos \wp_{\mathfrak{w}_i, \mathfrak{w}_j} \right). \tag{29}$$

Wherein $\mathfrak{w}_i$ is MF-vector from i^{th} row of relation matrix, and $\wp_{\mathfrak{w}_i,\mathfrak{w}_j}$ is the relation angle between $\mathfrak{w}_i$ and $\mathfrak{w}_j$. Then, the normalized relation angles are obtained regarding to molecular geometry shapes using Equations (30) – (35) (Shen et al., 2025).

$$\backslash\wp^{general}_{\mathfrak{w}_i,\mathfrak{w}_j} = \frac{\wp_{\mathfrak{w}_i,\mathfrak{w}_j}}{\max\left(\wp_{\mathfrak{w}_i,\mathfrak{w}_j}\right)}. \tag{30}$$

$$\backslash\wp^{linear}_{\mathfrak{w}_i,\mathfrak{w}_j} = \frac{\wp_{\mathfrak{w}_i,\mathfrak{w}_j}}{\pi}. \tag{31}$$

$$\backslash\wp^{trigonal\ planar}_{\mathfrak{w}_i,\mathfrak{w}_j} = \frac{\wp_{\mathfrak{w}_i,\mathfrak{w}_j}}{\left(\frac{2\pi}{3}\right)}. \tag{32}$$

$$\backslash\wp^{tetrahedral}_{\mathfrak{w}_i,\mathfrak{w}_j} = \frac{\wp_{\mathfrak{w}_i,\mathfrak{w}_j}}{\left(\frac{\pi}{2}\right)}. \tag{33}$$

$$\backslash\wp^{trigonal\ bipyramidal}_{\mathfrak{w}_i,\mathfrak{w}_j} = \frac{\wp_{\mathfrak{w}_i,\mathfrak{w}_j}}{\left(\frac{2\pi}{5}\right)}. \tag{34}$$

$$\backslash\wp^{general}_{\mathfrak{w}_i,\mathfrak{w}_j} = \frac{\wp_{\mathfrak{w}_i,\mathfrak{w}_j}}{\left(\frac{\pi}{3}\right)}. \tag{35}$$

Afterwards, the reciprocal items are estimated by computing the inverse of these normalized relation angles according to multiplication as Equation (36).

$$r\wp^{\sim}_{\mathfrak{w}_i,\mathfrak{w}_j} = \frac{1}{\backslash\wp^{\sim}_{\mathfrak{w}_i,\mathfrak{w}_j}}. \tag{36}$$

Later, these items are normalized, and a normalization relation matrix is created that accepts these normalized items as elements by Equations (37) and (38).

$$\mathfrak{n}_{ij} = \frac{r\wp^{\sim}_{\mathfrak{w}_i,\mathfrak{w}_j}}{\sum r\wp^{\sim}_{\mathfrak{w}_i,\mathfrak{w}_j}}. \tag{37}$$

$$N = \left[\mathfrak{n}_{ij}\right]. \tag{38}$$

After creating this matrix, natural logarithms are estimated with Equations (39) and (40).

$$\ln\left(\mathfrak{n}_{ij}\right) \approx \ln\left(\mathfrak{n}_i\right) - \ln\left(\mathfrak{n}_j\right). \tag{39}$$

$$\ln\left(\mathfrak{n}_{ij}\right) \approx \mathfrak{z}_i - \mathfrak{z}_j. \tag{40}$$

Wherein $\mathfrak{n}_{ij}$ is the item of normalization relation matrix. After that, the linear equation system is set in Equation (41).

$$\mathfrak{n}_{n1}\mathfrak{z}_1 + \mathfrak{n}_{n2}\mathfrak{z}_2 + \ldots + \mathfrak{n}_{nn}\mathfrak{z}_n = \mathfrak{b}_n. \tag{41}$$

This system contains n equations. The system is solved by Equations (42) - (44).

$$\mathfrak{n}^T\mathfrak{n}\mathfrak{z} = \mathfrak{n}^T\mathfrak{b} \tag{42}$$

$$\left(\mathfrak{n}^T\mathfrak{n}\right)_{ij} = \sum_{k=1}^{m} \mathfrak{z}_{ki}\mathfrak{z}_{kj}. \tag{43}$$

$$\left(\mathfrak{n}^T\mathfrak{b}\right)_{i} = \sum_{k=1}^{m} \mathfrak{z}_{ki}\mathfrak{b}_{k}. \tag{44}$$

Wherein $\mathfrak{n}^T$ is the coefficient matrix's transpose, and $\mathfrak{z}$ is the unknows' vector. Finally, the weight vector is obtained using Equation (45).

$$\mathfrak{x}_i = \frac{e^{\mathfrak{z}_i}}{\sum_{j=1}^{n} e^{\mathfrak{z}_j}}. \tag{45}$$

After obtaining the weight vector for criteria, the average of the assessment matrices related to the decision matrix formed in Equation (46) is computed by Equation (24).

$$D\mathcal{V} = [d\sqsubseteq_{ij}]_{m\times n}. \tag{46}$$

Next, the items of decision matrix are multiplied by the weight vector via Equation (47).

$$\mathcal{B} = \left(\mathfrak{x}_i\mathfrak{M}, \mathfrak{x}_i\mathfrak{N}, \mathfrak{x}_i\mathfrak{H}\right). \tag{47}$$

Then, each row of weighted decision matrix is defined as MF-vector as Equation (48).

$$\phi_i = \left[\left(\mathfrak{M}_{i1}, \mathfrak{N}_{i1}, \mathfrak{H}_{i1}\right), \left(\mathfrak{M}_{i2}, \mathfrak{N}_{i2}, \mathfrak{H}_{i2}\right), \ldots, \left(\mathfrak{M}_{im}, \mathfrak{N}_{im}, \mathfrak{H}_{im}\right)\right]. \tag{48}$$

Later, the weighted decision angle between each pair of MF-vectors is computed using Equations (49) – (52).

$$\left(\phi_i, \phi_j\right) = \sum_{l=1}^{n} \left(\mathfrak{M}_{i,l}\mathfrak{M}_{j,l} + \mathfrak{N}_{i,l}\mathfrak{N}_{j,l} + \mathfrak{H}_{i,l}\mathfrak{H}_{j,l}\right). \tag{49}$$

$$\left\|\phi_i\right\| = \sum_{l=1}^{m} \left(\mathfrak{M}_{i,l}^2 + \mathfrak{N}_{i,l}^2 + \mathfrak{H}_{i,l}^2\right). \tag{50}$$

$$\cos \mathfrak{Z}_{\phi_i,\phi_j} = \frac{\left(\phi_i, \phi_j\right)}{\left\|\phi_i\right\| \left\|\phi_j\right\|}. \tag{51}$$

$$\mathfrak{Z}_{\phi_i,\phi_j} = \cos^{-1}\ \left(\cos \mathfrak{Z}_{\phi_i,\phi_j}\right). \tag{52}$$

Wherein ϕ_i is MF-vector from i^{th} row of weighted decision matrix, and $\mathfrak{Z}_{\phi_i,\phi_j}$ is the weighted decision angle between ϕ_i and ϕ_j. The number of alternatives is m. Then, the normalized weighted decision angles are obtained regarding to molecular geometry shapes using Equations (53) – (58).

$$\backslash\mathfrak{Z}_{\phi_i,\phi_j}^{general} = \frac{\mathfrak{Z}_{\phi_i,\phi_j}}{\max\left(\mathfrak{Z}_{\phi_i,\phi_j}\right)}. \tag{53}$$

$$\backslash \mathfrak{Z}_{\phi_i,\phi_j}^{linear} = \frac{\mathfrak{Z}_{\phi_i,\phi_j}}{\pi}. \tag{54}$$

$$\backslash \mathfrak{Z}_{\phi_i,\phi_j}^{trigonal\ planar} = \frac{\mathfrak{Z}_{\phi_i,\phi_j}}{\left(\frac{2\pi}{3}\right)}. \tag{55}$$

$$\backslash \mathfrak{Z}_{\phi_i,\phi_j}^{tetrahedral} = \frac{\mathfrak{Z}_{\phi_i,\phi_j}}{\left(\frac{\pi}{2}\right)}. \tag{56}$$

$$\backslash \mathfrak{Z}_{\phi_i,\phi_j}^{trigonal\ bipyramidal} = \frac{\mathfrak{Z}_{\phi_i,\phi_j}}{\left(\frac{2\pi}{5}\right)}. \tag{57}$$

$$\backslash \mathfrak{Z}_{\phi_i,\phi_j}^{ortahedral} = \frac{\mathfrak{Z}_{\phi_i,\phi_j}}{\left(\frac{\pi}{3}\right)}. \tag{58}$$

Afterwards, the reciprocal items are estimated by computing the inverse of these normalized weighted decision angles according to multiplication according to Equation (59).

$$r\mathfrak{Z}_{\phi_i,\phi_j}^{\sim} = \frac{1}{\backslash \mathfrak{Z}_{\phi_i,\phi_j}^{\sim}}. \tag{59}$$

Later, these items are normalized by Equation (60), and a final decision matrix formed in Equation (61) is generated that accepts these normalized items as elements.

$$f_{ij} = \frac{r\mathfrak{Z}_{\phi_i,\phi_j}^{\sim}}{\sum_{j=1}^{n} r\mathfrak{Z}_{\phi_i,\phi_j}^{\sim}}. \tag{60}$$

$$F = [f_{ij}]. \tag{61}$$

The particle presentation is identified as a vector for potential results in Equation (62).

$$\mathbb{X}_i = \{\curvearrowleft_{i1}, \curvearrowleft_{i2}, \ldots, \curvearrowleft_{in}\}. \tag{62}$$

Wherein $\curvearrowleft$ the decision position. After that, the velocities for particles are calculated by Equation (63).

$$\mathbb{V}_{ij}(t+1) = 0.5\mathbb{V}_{ij}(t) + 1.5r_1\left(P_{ij}(t) - \mathbb{X}_{ij}(t)\right) + 1.5r_2\left(P_{gb_j}(t) - \mathbb{X}_{ij}(t)\right) \tag{63}$$

Wherein the values of r are random numbers between 0 and 1, and $\mathbb{V}_{ij}(t)$ is the updated volatility degree. The initial velocity is defined in Equation (64).

$$\mathbb{V}_{ij}(1) = 0.1\left(P_{\max_i} - P_{\min_i}\right)\nabla. \tag{64}$$

Wherein $\nabla \in [-1, 1]$. After identifying these definitions, the updated positions of particles are computed with Equation (65) until the absolute difference between the personal and global best positions is lower than .001. In other words, Equations (66) – (69) are used for testing.

$$\mathbb{X}_{ij}(t+1) = \mathbb{X}_{ij}(t) + \mathbb{V}_{ij}(t+1). \tag{65}$$

$$P_{ij}(t+1) = Best\left(P_{ij}(t),\ \mathbb{X}_{ij}(t+1)\right). \tag{66}$$

$$P_{gb_j}(t+1) = Best\left(P_{gb_j}(t),\ \{\mathbb{X}_{ij}(t+1)\}\ \ all\ i\right). \tag{67}$$

$$\Delta = P_{gb_j}(t+1) - P_{gb_j}(t). \tag{68}$$

$$|\Delta| < .001. \tag{69}$$

Finally, the average item for each item is obtained and used for ranking using Equation (70).

$$\frac{1}{n}\sum_{i=1}^{n} P_{ij}. \tag{70}$$

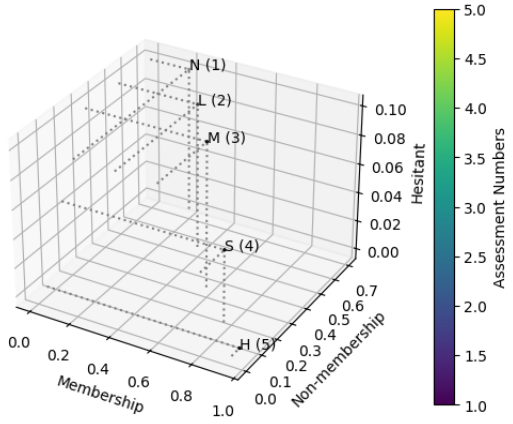
4 Analysis results

Assessments of transparent solar panel installations in buildings are presented in this section with tables, figures and matrices along with explanations.

4.1 Obtaining the weights of experts

At the beginning of the Entropy-game expert weighting, assessments for the relation matrix from experts are collected. The investment criteria are identified as energy regulations (REGL), architectural aesthetics (ARCH), return on investment (RTR), and regional solar irradiance (RGNL). In assessment process, the linguistic terms included negligible (N-1), low (L-2), moderate (M-3), significant (S-4), and high (H-5) with assessment numbers are used. The linguistic variables' 3D visualization is shown in Figure 2.

Figure 2: 3D of MFNs



After that, criteria are evaluated by experts. The experts' assessments for relation matrix are shared in Table 1.

Table 1: Assessments for Relation Matrix

E1	**REGL**	**ARCH**	**RTRN**	**RGNL**
REGL		M	H	S
ARCH	S		S	H
RTRN	S	S		S
RGNL	H	S	S	
E2	**REGL**	**ARCH**	**RTRN**	**RGNL**
REGL		H	H	H
ARCH	S		S	H
RTRN	S	S		H
RGNL	S	H	S	
E3	**REGL**	**ARCH**	**RTRN**	**RGNL**
REGL		M	H	H
ARCH	S		S	H
RTRN	S	S		H
RGNL	S	M	S	

These linguistic terms in Table 1 are converted to assessments numbers and Equation (13) is used for normalization of relation matrices. The normalized relation matrices of experts are illustrated in Table 2.

Table 2: Normalized Relation Matrices

E1	**REGL**	**ARCH**	**RTRN**	**RGNL**
REGL		.273	.385	.308
ARCH	.308		.308	.385
RTRN	.308	.364		.308
RGNL	.385	.364	.308	
E2	**REGL**	**ARCH**	**RTRN**	**RGNL**
REGL		.357	.385	.333
ARCH	.333		.308	.333
RTRN	.333	.286		.333
RGNL	.333	.357	.308	
E3	**REGL**	**ARCH**	**RTRN**	**RGNL**
REGL		.300	.385	.333
ARCH	.333		.308	.333
RTRN	.333	.400		.333
RGNL	.333	.300	.308	

Afterwards, consistency-adjusted, coalition and Shapley parameters are computed using Equations (15) - (17), respectively. All parameters are summarized in Table 3.

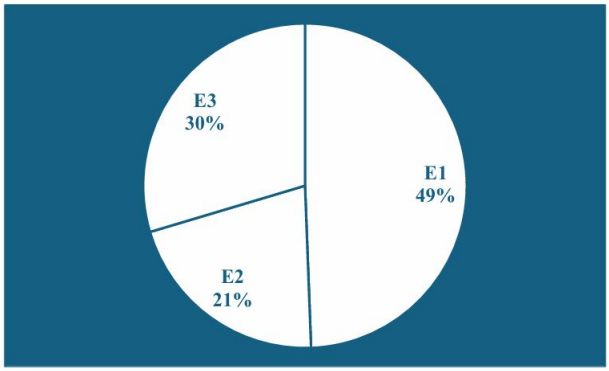
Table 3: Parameters

	$\rfloor\!\dashv$	$\rfloor\!\sqsubseteq$	$\int\!\sqsubseteq$
E1	.006	.024	.016
E2	.003	.010	.007
E3	.004	.014	.009

Finally, the overall weight vector is obtained with the help of Equation (18). This vector is shown in Figure 3.

According to weight vector in Figure 3, the most successful expert is E1. In this case, the penalty factor for the $\mathcal{Q}$-learning algorithm is 0.494. The other elements of the vector are used as reward factors. In addition, the MF

Figure 3: Weight Vector



assessments of E1 are defined as $\mathcal{Q}_{s,a}^{mse}$.

4.2 Creating the balanced assessment matrices

Similarly, the alternative investment policies for transparent solar panel installations are determined such as solar-integrated smart windows (SWNDW), transparent solar roofing (TRANS), solar bus shelters (BUSSH), solar atriums and canopies (ATRCN), and solar-powered glass walkways (GLSWW). The assessments for decision matrix are given in Table 4.

Table 4: Assessments for Decision Matrix

E1	**REGL**	**ARCH**	**RTRN**	**RGNL**
SWNDW	H	M	H	H
TRANS	H	M	S	S
BUSSH	H	H	S	S
ATRCN	S	S	H	S
GLSWW	M	H	S	S
E2	**REGL**	**ARCH**	**RTRN**	**RGNL**
SWNDW	H	H	H	H
TRANS	H	H	S	S
BUSSH	H	H	S	S
ATRCN	S	S	H	M
GLSWW	M	H	S	S
E3	**REGL**	**ARCH**	**RTRN**	**RGNL**
SWNDW	H	S	H	H
TRANS	H	S	S	S
BUSSH	S	H	S	S
ATRCN	S	S	H	S
GLSWW	S	H	S	S

The assessments in Table 1 and Table 4 are transformed into MFNs. The reward-penalty degrees among the most successful expert and others are constructed with Equations (19) and (20). The $\mathcal{RD}$ of relation and decision matrices is illustrated in Table 5 and Table 6.

Table 5: $\mathcal{RD}$ **Matrices for Relation**

E1-E2	**REGL**	**ARCH**	**RTRN**	**RGNL**
REGL	(.00, .00, .00)	(.07, -.05, -.02)	(.00, .00, .00)	(.03, -.02, -.01)
ARCH	(.00, .00, .00)	(.00, .00, .00)	(.00, .00, .00)	(.00, .00, .00)
RTRN	(.00, .00, .00)	(.00, .00, .00)	(.00, .00, .00)	(.03, -.02, -.01)
RGNL	(-.03, .02, .01)	(.03, -.02, -.01)	(.00, .00, .00)	(.00, .00, .00)
E1-E3	**REGL**	**ARCH**	**RTRN**	**RGNL**
REGL	(.00, .00, .00)	(.00, .00, .00)	(.00, .00, .00)	(.04, -.03, -.01)
ARCH	(.00, .00, .00)	(.00, .00, .00)	(.00, .00, .00)	(.00, .00, .00)
RTRN	(.00, .00, .00)	(.00, .00, .00)	(.00, .00, .00)	(.04, -.03, -.01)
RGNL	(-.04, .03, .01)	(-.06, .04, .01)	(.00, .00, .00)	(.00, .00, .00)

Table 6: $\mathcal{RD}$ **Matrices for Decision**

E1-E2	**REGL**	**ARCH**	**RTRN**	**RGNL**
SWNDW	(.00, .00, .00)	(.07, -.05, -.02)	(.00, .00, .00)	(.00, .00, .00)
TRANS	(.00, .00, .00)	(.07, -.05, -.02)	(.00, .00, .00)	(.00, .00, .00)
BUSSH	(.00, .00, .00)	(.00, .00, .00)	(.00, .00, .00)	(.00, .00, .00)
ATRCN	(.00, .00, .00)	(.00, .00, .00)	(.00, .00, .00)	(-.04, .03, .01)
GLSWW	(.00, .00, .00)	(.00, .00, .00)	(.00, .00, .00)	(.00, .00, .00)
E1-E3	**REGL**	**ARCH**	**RTRN**	**RGNL**
SWNDW	(.00, .00, .00)	(.06, -.04, -.01)	(.00, .00, .00)	(.00, .00, .00)
TRANS	(.00, .00, .00)	(.06, -.04, -.01)	(.00, .00, .00)	(.00, .00, .00)
BUSSH	(-.04, .03, .01)	(.00, .00, .00)	(.00, .00, .00)	(.00, .00, .00)
ATRCN	(.00, .00, .00)	(.00, .00, .00)	(.00, .00, .00)	(.00, .00, .00)
GLSWW	(.06, -.04, -.01)	(.00, .00, .00)	(.00, .00, .00)	(.00, .00, .00)

Similarly, the $\mathcal{PD}$ of two matrices is displayed in Table 7 and Table 8.

Table 7: $\mathcal{RD}$ **Matrices for Relation**

E1-E2	**REGL**	**ARCH**	**RTRN**	**RGNL**
REGL	(.00, .00, .00)	(-.17, .12, .05)	(.00, .00, .00)	(-.07, .05, .02)
ARCH	(.00, .00, .00)	(.00, .00, .00)	(.00, .00, .00)	(.00, .00, .00)
RTRN	(.00, .00, .00)	(.00, .00, .00)	(.00, .00, .00)	(-.07, .05, .02)
RGNL	(.07, -.05, -.02)	(-.07, .05, .02)	(.00, .00, .00)	(.00, .00, .00)
E1-E3	**REGL**	**ARCH**	**RTRN**	**RGNL**
REGL	(.00, .00, .00)	(.00, .00, .00)	(.00, .00, .00)	(-.07, .05, .02)
ARCH	(.00, .00, .00)	(.00, .00, .00)	(.00, .00, .00)	(.00, .00, .00)

Table 8: $\mathcal{RD}$ Matrices for Decision

E1-E2	**REGL**	**ARCH**	**RTRN**	**RGNL**
SWNDW	(.00, .00, .00)	(-.17, .12, .05)	(.00, .00, .00)	(.00, .00, .00)
TRANS	(.00, .00, .00)	(-.17, .12, .05)	(.00, .00, .00)	(.00, .00, .00)
BUSSH	(.00, .00, .00)	(.00, .00, .00)	(.00, .00, .00)	(.00, .00, .00)
ATRCN	(.00, .00, .00)	(.00, .00, .00)	(.00, .00, .00)	(.10, -.07, -.02)
GLSWW	(.00, .00, .00)	(.00, .00, .00)	(.00, .00, .00)	(.00, .00, .00)
E1-E3	**REGL**	**ARCH**	**RTRN**	**RGNL**
SWNDW	(.00, .00, .00)	(-.10, .07, .02)	(.00, .00, .00)	(.00, .00, .00)
TRANS	(.00, .00, .00)	(-.10, .07, .02)	(.00, .00, .00)	(.00, .00, .00)
BUSSH	(.07, -.05, -.02)	(.00, .00, .00)	(.00, .00, .00)	(.00, .00, .00)
ATRCN	(.00, .00, .00)	(.00, .00, .00)	(.00, .00, .00)	(.00, .00, .00)
GLSWW	(-.10, .07, .02)	(.00, .00, .00)	(.00, .00, .00)	(.00, .00, .00)

Using reward-penalty degrees, assessment matrices of others are updated according to the most successful expert using Equation (21). By { = .1, the updated assessment matrices are exhibited in Table 9 and Table 10.

Table 9: Updated Matrices (=0.1) for Relation

E1-E2	**REGL**	**ARCH**	**RTRN**	**RGNL**
REGL	(.00, .00, .00)	(.62, .28, .09)	(.95, .05, .00)	(.81, .14, .05)
ARCH	(.80, .15, .05)	(.00, .00, .00)	(.80, .15, .05)	(.95, .05, .00)
RTRN	(.80, .15, .05)	(.80, .15, .05)	(.00, .00, .00)	(.81, .14, .05)
RGNL	(.94, .06, .00)	(.81, .14, .05)	(.80, .15, .05)	(.00, .00, .00)
E1-E3	**REGL**	**ARCH**	**RTRN**	**RGNL**
REGL	(.00, .00, .00)	(.60, .30, .10)	(.95, .05, .00)	(.81, .14, .05)
ARCH	(.80, .15, .05)	(.00, .00, .00)	(.80, .15, .05)	(.95, .05, .00)
RTRN	(.80, .15, .05)	(.80, .15, .05)	(.00, .00, .00)	(.81, .14, .05)
RGNL	(.94, .06, .00)	(.78, .16, .05)	(.80, .15, .05)	(.00, .00, .00)

Table 10: Updated Matrices ({ = .**1**) for Decision

E1-E2	**REGL**	**ARCH**	**RTRN**	**RGNL**
SWNDW	(.95, .05, .00)	(.62, .28, .09)	(.95, .05, .00)	(.95, .05, .00)
TRANS	(.95, .05, .00)	(.62, .28, .09)	(.80, .15, .05)	(.80, .15, .05)
BUSSH	(.95, .05, .00)	(.95, .05, .00)	(.80, .15, .05)	(.80, .15, .05)
ATRCN	(.80, .15, .05)	(.80, .15, .05)	(.95, .05, .00)	(.79, .16, .05)
GLSWW	(.60, .30, .10)	(.95, .05, .00)	(.80, .15, .05)	(.80, .15, .05)
E1-E3	**REGL**	**ARCH**	**RTRN**	**RGNL**
SWNDW	(.95, .05, .00)	(.62, .29, .10)	(.95, .05, .00)	(.95, .05, .00)
TRANS	(.95, .05, .00)	(.62, .29, .10)	(.80, .15, .05)	(.80, .15, .05)
BUSSH	(.94, .06, .00)	(.95, .05, .00)	(.80, .15, .05)	(.80, .15, .05)
ATRCN	(.80, .15, .05)	(.80, .15, .05)	(.95, .05, .00)	(.80, .15, .05)
GLSWW	(.62, .29, .10)	(.95, .05, .00)	(.80, .15, .05)	(.80, .15, .05)

Since the convergence condition is not met at this stage, the iteration is continued. The threshold value is 0.02. First iteration's results are shown in Table 11 and Table 12.

Table 11: Absolute Differences for Relation (First Iteration)

E1-E2	**REGL**	**ARCH**	**RTRN**	**RGNL**
REGL	(.000, .000, .000)	(.025, .018, .007)	(.000, .000, .000)	(.011, .007, .004)
ARCH	(.000, .000, .000)	(.000, .000, .000)	(.000, .000, .000)	(.000, .000, .000)
RTRN	(.000, .000, .000)	(.000, .000, .000)	(.000, .000, .000)	(.011, .007, .004)
RGNL	(.011, .007, .004)	(.011, .007, .004)	(.000, .000, .000)	(.000, .000, .000)
E1-E3	**REGL**	**ARCH**	**RTRN**	**RGNL**
REGL	(.000, .000, .000)	(.000, .000, .000)	(.000, .000, .000)	(.012, .008, .004)
ARCH	(.000, .000, .000)	(.000, .000, .000)	(.000, .000, .000)	(.000, .000, .000)
RTRN	(.000, .000, .000)	(.000, .000, .000)	(.000, .000, .000)	(.012, .008, .004)
RGNL	(.012, .008, .004)	(.016, .012, .004)	(.000, .000, .000)	(.000, .000, .000)

Table 12: Absolute Differences for Decision (First Iteration)

E1-E2	**REGL**	**ARCH**	**RTRN**	**RGNL**
SWNDW	(.000, .000, .000)	(.025, .018, .007)	(.000, .000, .000)	(.000, .000, .000)
TRANS	(.000, .000, .000)	(.025, .018, .007)	(.000, .000, .000)	(.000, .000, .000)
BUSSH	(.000, .000, .000)	(.000, .000, .000)	(.000, .000, .000)	(.000, .000, .000)
ATRCN	(.000, .000, .000)	(.000, .000, .000)	(.000, .000, .000)	(.014, .011, .004)
GLSWW	(.000, .000, .000)	(.000, .000, .000)	(.000, .000, .000)	(.000, .000, .000)
E1-E3	**REGL**	**ARCH**	**RTRN**	**RGNL**
SWNDW	(.000, .000, .000)	(.016, .012, .004)	(.000, .000, .000)	(.000, .000, .000)
TRANS	(.000, .000, .000)	(.016, .012, .004)	(.000, .000, .000)	(.000, .000, .000)
BUSSH	(.012, .008, .004)	(.000, .000, .000)	(.000, .000, .000)	(.000, .000, .000)
ATRCN	(.000, .000, .000)	(.000, .000, .000)	(.000, .000, .000)	(.000, .000, .000)
GLSWW	(.016, .012, .004)	(.000, .000, .000)	(.000, .000, .000)	(.000, .000, .000)

Other iterations' results are shared in Table 13 and Table 14.

Table 13: Iterative Results (Relation)

Iteration 2				
E1-E2	**REGL**	**ARCH**	**RTRN**	**RGNL**
REGL	(.000, .000, .000)	(.023, .016, .007)	(.000, .000, .000)	(.010, .007, .003)
ARCH	(.000, .000, .000)	(.000, .000, .000)	(.000, .000, .000)	(.000, .000, .000)
RTRN	(.000, .000, .000)	(.000, .000, .000)	(.000, .000, .000)	(.010, .007, .003)
RGNL	(.010, .007, .003)	(.010, .007, .003)	(.000, .000, .000)	(.000, .000, .000)
Iteration 3				
E1-E2	**REGL**	**ARCH**	**RTRN**	**RGNL**
REGL	(.000, .000, .000)	(.021, .015, .006)	(.000, .000, .000)	(.009, .006, .003)
ARCH	(.000, .000, .000)	(.000, .000, .000)	(.000, .000, .000)	(.000, .000, .000)
RTRN	(.000, .000, .000)	(.000, .000, .000)	(.000, .000, .000)	(.009, .006, .003)
Iteration 2				
RGNL	(.009, .006, .003)	(.009, .006, .003)	(.000, .000, .000)	(.000, .000, .000)
Iteration 4				
E1-E2	**REGL**	**ARCH**	**RTRN**	**RGNL**
REGL	(.000, .000, .000)	(.020, .014, .006)	(.000, .000, .000)	(.008, .006, .003)
ARCH	(.000, .000, .000)	(.000, .000, .000)	(.000, .000, .000)	(.000, .000, .000)
RTRN	(.000, .000, .000)	(.000, .000, .000)	(.000, .000, .000)	(.008, .006, .003)
RGNL	(.008, .006, .003)	(.008, .006, .003)	(.000, .000, .000)	(.000, .000, .000)

Table 14: Iterative Results (Decision)

Iteration 2				
E1-E2	**REGL**	**ARCH**	**RTRN**	**RGNL**
SWNDW	(.000, .000, .000)	(.023, .016, .007)	(.000, .000, .000)	(.000, .000, .000)
TRANS	(.000, .000, .000)	(.023, .016, .007)	(.000, .000, .000)	(.000, .000, .000)
BUSSH	(.000, .000, .000)	(.000, .000, .000)	(.000, .000, .000)	(.000, .000, .000)
ATRCN	(.000, .000, .000)	(.000, .000, .000)	(.000, .000, .000)	(.013, .010, .003)
GLSWW	(.000, .000, .000)	(.000, .000, .000)	(.000, .000, .000)	(.000, .000, .000)
Iteration 3				
E1-E2	**REGL**	**ARCH**	**RTRN**	**RGNL**
SWNDW	(.000, .000, .000)	(.021, .015, .006)	(.000, .000, .000)	(.000, .000, .000)
TRANS	(.000, .000, .000)	(.021, .015, .006)	(.000, .000, .000)	(.000, .000, .000)
BUSSH	(.000, .000, .000)	(.000, .000, .000)	(.000, .000, .000)	(.000, .000, .000)
ATRCN	(.000, .000, .000)	(.000, .000, .000)	(.000, .000, .000)	(.012, .009, .003)
GLSWW	(.000, .000, .000)	(.000, .000, .000)	(.000, .000, .000)	(.000, .000, .000)
Iteration 4				
Iteration 2				
E1-E2	**REGL**	**ARCH**	**RTRN**	**RGNL**
SWNDW	(.000, .000, .000)	(.020, .014, .006)	(.000, .000, .000)	(.000, .000, .000)
TRANS	(.000, .000, .000)	(.020, .014, .006)	(.000, .000, .000)	(.000, .000, .000)
BUSSH	(.000, .000, .000)	(.000, .000, .000)	(.000, .000, .000)	(.000, .000, .000)
ATRCN	(.000, .000, .000)	(.000, .000, .000)	(.000, .000, .000)	(.011, .008, .003)
GLSWW	(.000, .000, .000)	(.000, .000, .000)	(.000, .000, .000)	(.000, .000, .000)

Four iterations are performed so that the maximum of absolute difference is less than this threshold value. The end of fourth iteration, balanced assessment matrices are obtained. The balanced matrices are presented in Table 15 and Table 16.

Table 15: Balanced Matrices for Relation

Balanced Relation Matrices				
E1	**REGL**	**ARCH**	**RTRN**	**RGNL**
REGL	(.00, .00, .00)	(.67, .25, .08)	(.95, .05, .00)	(.83, .13, .04)
ARCH	(.80, .15, .05)	(.00, .00, .00)	(.80, .15, .05)	(.95, .05, .00)
RTRN	(.80, .15, .05)	(.80, .15, .05)	(.00, .00, .00)	(.83, .13, .04)
RGNL	(.92, .07, .01)	(.83, .13, .04)	(.80, .15, .05)	(.00, .00, .00)
E2	**REGL**	**ARCH**	**RTRN**	**RGNL**
REGL	(.00, .00, .00)	(.95, .05, .00)	(.95, .05, .00)	(.95, .05, .00)
ARCH	(.80, .15, .05)	(.00, .00, .00)	(.80, .15, .05)	(.95, .05, .00)
RTRN	(.80, .15, .05)	(.80, .15, .05)	(.00, .00, .00)	(.95, .05, .00)
RGNL	(.80, .15, .05)	(.95, .05, .00)	(.80, .15, .05)	(.00, .00, .00)
E3	**REGL**	**ARCH**	**RTRN**	**RGNL**
REGL	(.00, .00, .00)	(.60, .30, .10)	(.95, .05, .00)	(.95, .05, .00)
ARCH	(.80, .15, .05)	(.00, .00, .00)	(.80, .15, .05)	(.95, .05, .00)
RTRN	(.80, .15, .05)	(.80, .15, .05)	(.00, .00, .00)	(.95, .05, .00)
RGNL	(.80, .15, .05)	(.60, .30, .10)	(.80, .15, .05)	(.00, .00, .00)

Table 16: Balanced Matrices for Decision

Balanced Decision Matrices				
E1	**REGL**	**ARCH**	**RTRN**	**RGNL**
SWNDW	(.95, .05, .00)	(.67, .25, .08)	(.95, .05, .00)	(.95, .05, .00)
TRANS	(.95, .05, .00)	(.67, .25, .08)	(.80, .15, .05)	(.80, .15, .05)
BUSSH	(.95, .05, .00)	(.95, .05, .00)	(.80, .15, .05)	(.80, .15, .05)
ATRCN	(.80, .15, .05)	(.80, .15, .05)	(.95, .05, .00)	(.76, .18, .06)
GLSWW	(.60, .30, .10)	(.95, .05, .00)	(.80, .15, .05)	(.80, .15, .05)
E2	**REGL**	**ARCH**	**RTRN**	**RGNL**
SWNDW	(.95, .05, .00)	(.95, .05, .00)	(.95, .05, .00)	(.95, .05, .00)
TRANS	(.95, .05, .00)	(.95, .05, .00)	(.80, .15, .05)	(.80, .15, .05)
BUSSH	(.95, .05, .00)	(.95, .05, .00)	(.80, .15, .05)	(.80, .15, .05)
ATRCN	(.80, .15, .05)	(.80, .15, .05)	(.95, .05, .00)	(.60, .30, .10)
GLSWW	(.60, .30, .10)	(.95, .05, .00)	(.80, .15, .05)	(.80, .15, .05)
E3	**REGL**	**ARCH**	**RTRN**	**RGNL**
SWNDW	(.95, .05, .00)	(.80, .15, .05)	(.95, .05, .00)	(.95, .05, .00)
TRANS	(.95, .05, .00)	(.80, .15, .05)	(.80, .15, .05)	(.80, .15, .05)
BUSSH	(.80, .15, .05)	(.95, .05, .00)	(.80, .15, .05)	(.80, .15, .05)
ATRCN	(.80, .15, .05)	(.80, .15, .05)	(.95, .05, .00)	(.80, .15, .05)
GLSWW	(.80, .15, .05)	(.95, .05, .00)	(.80, .15, .05)	(.80, .15, .05)

While the relation matrices in Table 11 and Table 12 are used for LSO analysis, decision matrices are used for MOPSO.

4.3 Computing weight vector of the investment criteria set for transparent solar panel installations in buildings

At the beginning of the LSO, the average of the assessment matrices related to the relation matrix in Table 15 is calculated by Equation (24). The averaged numbers are illustrated in Table 17.

Table 17: Averaged Numbers

	REGL	**ARCH**	**RTRN**	**RGNL**
REGL	(.00, .00, .00)	(.74, .20, .06)	(.95, .05, .00)	(.91, .08, .01)
ARCH	(.80, .15, .05)	(.00, .00, .00)	(.80, .15, .05)	(.95, .05, .00)
RTRN	(.80, .15, .05)	(.80, .15, .05)	(.00, .00, .00)	(.91, .08, .01)
RGNL	(.84, .12, .04)	(.79, .16, .05)	(.80, .15, .05)	(.00, .00, .00)

Next, each row of relation matrix exiting the diagonal values is defined as MF-vector. Because these values are empty. Table 18 shows relation vectors.

Table 18: Relation Vector

	Relation
$\mathfrak{w}_1$	[(.74, .20, .06), (.95, .05, .00), (.91, .08, .01)]
$\mathfrak{w}_2$	[(.80, .15, .05), (.80, .15, .05), (.95, .05, .00)]
$\mathfrak{w}_3$	[(.80, .15, .05), (.80, .15, .05), (.91, .08, .01)]
$\mathfrak{w}_4$	[(.84, .12, .04), (.79, .16, .05), (.80, .15, .05)]

Then, dot products are computed and given in Table 19.

Table 19: Dot Products between Relation Vectors

	$\mathfrak{w}_1$	$\mathfrak{w}_2$	$\mathfrak{w}_3$	$\mathfrak{w}_4$
$\mathfrak{w}_1$		2.260	2.226	2.150
$\mathfrak{w}_2$	2.260		2.198	2.121
$\mathfrak{w}_3$	2.226	2.198		2.093
$\mathfrak{w}_4$	2.150	2.121	2.093	

Using the dot product values and magnitudes of vectors, the cosines of angles are calculated. The results are illustrated in Table 20.

Table 20: Cosines of Relation Angles

	$\mathbf{cos}(\wp_{\mathfrak{w}_1})$	$\mathbf{cos}(\wp_{\mathfrak{w}_2})$	$\mathbf{cos}(\wp_{\mathfrak{w}_3})$	$\mathbf{cos}(\wp_{\mathfrak{w}_4})$
$cos(\wp_{\mathfrak{w}_1})$		.991	.991	.985
$cos(\wp_{\mathfrak{w}_2})$	.991		1.000	.992
$cos(\wp_{\mathfrak{w}_3})$	.991	1.000		.995
$cos(\wp_{\mathfrak{w}_4})$	.985	.992	.995	

Later, the relation angle between each pair of MF-vectors is computed using Equation (29). The relation angles are displayed in Table 21.

Table 21: Relation Angles

	$\wp_{\mathfrak{w}_1}$	$\wp_{\mathfrak{w}_2}$	$\wp_{\mathfrak{w}_3}$	$\wp_{\mathfrak{w}_4}$
$\wp_{\mathfrak{w}_1}$		.137	.131	.173
$\wp_{\mathfrak{w}_2}$	.137		.030	.125
$\wp_{\mathfrak{w}_3}$	.131	.030		.097
$\wp_{\mathfrak{w}_4}$	.173	.125	.097	

Then, the normalized relation angles are obtained regarding to molecular geometry shapes using Equations (30) – (35). The normalized relation angles are shared in Table 22.

Table 22: Normalized Relation Angles

Linear	$\wp_{\mathfrak{w}_1}$	$\wp_{\mathfrak{w}_2}$	$\wp_{\mathfrak{w}_3}$	$\wp_{\mathfrak{w}_4}$
$\wp_{\mathfrak{w}_1}$	.000	.044	.042	.055
$\wp_{\mathfrak{w}_2}$	.044	.000	.009	.040
$\wp_{\mathfrak{w}_3}$	.042	.009	.000	.031
$\wp_{\mathfrak{w}_4}$	.055	.040	.031	.000
Trigonal Planar	$\wp_{\mathfrak{w}_1}$	$\wp_{\mathfrak{w}_2}$	$\wp_{\mathfrak{w}_3}$	$\wp_{\mathfrak{w}_4}$
$\wp_{\mathfrak{w}_1}$	.000	.065	.062	.082
$\wp_{\mathfrak{w}_2}$	.065	.000	.014	.060
$\wp_{\mathfrak{w}_3}$	.062	.014	.000	.046
$\wp_{\mathfrak{w}_4}$	.082	.060	.046	.000
Tetrahedral	$\wp_{\mathfrak{w}_1}$	$\wp_{\mathfrak{w}_2}$	$\wp_{\mathfrak{w}_3}$	$\wp_{\mathfrak{w}_4}$
$\wp_{\mathfrak{w}_1}$	.000	.072	.068	.090
$\wp_{\mathfrak{w}_2}$	.072	.000	.016	.066
$\wp_{\mathfrak{w}_3}$	.068	.016	.000	.051
$\wp_{\mathfrak{w}_4}$	.090	.066	.051	.000
Trigonal Bipyramidal	$\wp_{\mathfrak{w}_1}$	$\wp_{\mathfrak{w}_2}$	$\wp_{\mathfrak{w}_3}$	$\wp_{\mathfrak{w}_4}$
$\wp_{\mathfrak{w}_1}$	.000	.075	.071	.094
$\wp_{\mathfrak{w}_2}$	.075	.000	.016	.068
$\wp_{\mathfrak{w}_3}$	.071	.016	.000	.053
$\wp_{\mathfrak{w}_4}$	.094	.068	.053	.000
Octahedral	$\wp_{\mathfrak{w}_1}$	$\wp_{\mathfrak{w}_2}$	$\wp_{\mathfrak{w}_3}$	$\wp_{\mathfrak{w}_4}$
$\wp_{\mathfrak{w}_1}$	.000	.087	.083	.110
$\wp_{\mathfrak{w}_2}$	.087	.000	.019	.080
$\wp_{\mathfrak{w}_3}$	.083	.019	.000	.062
$\wp_{\mathfrak{w}_4}$	.110	.080	.062	.000

Afterwards, the reciprocal items are estimated by computing the inverse of these normalized relation angles according to multiplication. The reciprocal items are displayed in Table 23.

Table 23: Reciprocal Items of Relation (Linear)

	$\mathbf{r}\wp_{\mathfrak{w}_1}$	$\mathbf{r}\wp_{\mathfrak{w}_2}$	$\mathbf{r}\wp_{\mathfrak{w}_3}$	$\mathbf{r}\wp_{\mathfrak{w}_4}$
$r\wp_{\mathfrak{w}_1}$		22.920	24.063	18.188
$r\wp_{\mathfrak{w}_2}$	22.920		105.933	25.109
$r\wp_{\mathfrak{w}_3}$	24.063	105.933		32.418
	$\mathbf{r}\wp_{\mathfrak{w}_1}$	$\mathbf{r}\wp_{\mathfrak{w}_2}$	$\mathbf{r}\wp_{\mathfrak{w}_3}$	$\mathbf{r}\wp_{\mathfrak{w}_4}$
$r\wp_{\mathfrak{w}_4}$	18.188	25.109	32.418	

Later, these items are normalized, and a normalization relation matrix is created that accepts these normalized items as elements. The normalization relation matrix for linear is summarized in Table 24.

Table 24: Normalization Relation Matrix (Linear)

	REGL	**ARCH**	**RTRN**	**RGNL**
REGL	0	.100	.105	.080
ARCH	.100	0	.463	.110
RTRN	.105	.463	0	.142
RGNL	.080	.110	.142	0

After creating the normalization relation matrix, natural logarithms are estimated with Equations (39) and (40). The logarithmic relation matrix for linear is illustrated in Table 25.

Table 25: Logarithmic Relation Matrix (Linear)

	REGL	**ARCH**	**RTRN**	**RGNL**
REGL		-2.300	-2.251	-2.531
ARCH	-2.300		-.769	-2.209
RTRN	-2.251	-.769		-1.953
RGNL	-2.531	-2.209	-1.953	

After that, the linear equation system is set in Equation (41). The system is given in Table 26.

Table 26: Linear Equation System

Equations	$\eth_1$	$\eth_2$	$\eth_3$	$\eth_4$	**Constants** ($\mathfrak{b}$)
1	3	-1	-1	-1	-7.083
2	-1	3	-1	-1	-.678
3	-1	-1	3	-1	1.067
4	-1	-1	-1	3	6.694

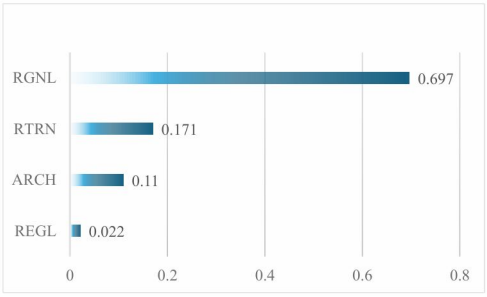
Equations in Table 14 are solved by Gaussian eliminations using Equations (42) – (44). Gaussian elimination iterations are presented in Table 27.

Table 27: Gaussian Eliminations

First Elimination					
	$\eth_1$	$\eth_2$	$\eth_3$	$\eth_4$	**Constants** ($\mathfrak{b}$)
1	1.000	-.333	-.333	-.333	-2.361
2	.000	2.667	-1.333	-1.333	-3.039
3	.000	-1.333	2.667	-1.333	-1.294
4	.000	-1.333	-1.333	2.667	4.333
Second Elimination					
	$\eth_1$	$\eth_2$	$\eth_3$	$\eth_4$	**Constants** ($\mathfrak{b}$)
1	1.000	-.333	-.333	-.333	-2.361
2	.000	1.000	-.500	-.500	-1.140
3	.000	.000	2.000	-2.000	-2.813
4	.000	.000	-2.000	2.000	2.813
Third Elimination					
	$\eth_1$	$\eth_2$	$\eth_3$	$\eth_4$	**Constants** ($\mathfrak{b}$)
1	1.000	-.333	-.333	-.333	-2.361
2	.000	1.000	-.500	-.500	-1.140
3	.000	.000	1.000	-1.000	-1.407
4	.000	.000	.000	.000	.000
Fourth Elimination					
	$\eth_1$	$\eth_2$	$\eth_3$	$\eth_4$	**Constants** ($\mathfrak{b}$)
1	1.000	-.333	-.333	-.333	-2.361
2	.000	1.000	-.500	-.500	-1.140
3	.000	.000	1.000	-1.000	-1.407
4	.000	.000	.000	1.000	1.000

Finally, the weight vector is obtained using Equation (45). The elements of weight vectors for linear are shown in Figure 4.

Figure 4: The Elements of Weight Vector (Linear)



As can be seen from the elements in Figure 4, the most effective investment criterion for transparent solar panel installations in buildings is regional solar irradiance. For consistency and validity of the results, analyses are performed again with all MGS and learning rates. The comparison of the priority order of the criteria is given in Table 28.

Table 28: Comparison of Priority Order of Criteria

$lr = .1$	**Linear**	**Trigonal Planar**	**Tetrahedral**	**Trigonal Bipyramidal**	**Octahedral**
REGL	4	4	4	4	4
ARCH	3	3	3	3	3
RTRN	2	2	2	2	2
RGNL	1	1	1	1	1
$lr = .5$	**Linear**	**Trigonal Planar**	**Tetrahedral**	**Trigonal Bipyramidal**	**Octahedral**
REGL	4	4	4	4	4
ARCH	3	3	3	3	3
RTRN	2	2	2	2	2
RGNL	1	1	1	1	1
$lr =$**1**	**Linear**	**Trigonal Planar**	**Tetrahedral**	**Trigonal Bipyramidal**	**Octahedral**
REGL	4	4	4	4	4
ARCH	3	3	3	3	3
RTRN	2	2	2	2	2
RGNL	1	1	1	1	1

When the orders in Table 28 are examined, it is seen that the results are consistent and valid. Because in all cases the results are the same.

4.4 Ranking of alternative investment policies for transparent solar panel installations

At the beginning of the MOPSO, the average of the assessment matrices related to the decision matrix in Table 16 is computed by Equation (24). The averaged items are displayed in Table 29.

Table 29: Averaged Items

	REGL	**ARCH**	**RTRN**	**RGNL**
SWNDW	(.95, .05, .00)	(.81, .15, .04)	(.95, .05, .00)	(.95, .05, .00)
TRANS	(.95, .05, .00)	(.81, .15, .04)	(.80, .15, .05)	(.80, .15, .05)
BUSSH	(.90, .08, .02)	(.95, .05, .00)	(.80, .15, .05)	(.80, .15, .05)
ATRCN	(.80, .15, .05)	(.80, .15, .05)	(.95, .05, .00)	(.72, .21, .07)
GLSWW	(.67, .25, .08)	(.95, .05, .00)	(.80, .15, .05)	(.80, .15, .05)

Next, the items of decision matrix are multiplied by the weight vector in Figure 3 via Equation (47). The weighted items are presented in Table 30.

Table 30: Weighted Items

	REGL	**ARCH**	**RTRN**	**RGNL**
SWNDW	(.02, .00, .00)	(.09, .02, .00)	(.16, .01, .00)	(.66, .03, .00)
TRANS	(.02, .00, .00)	(.09, .02, .00)	(.14, .03, .01)	(.56, .10, .03)
BUSSH	(.02, .00, .00)	(.10, .01, .00)	(.14, .03, .01)	(.56, .10, .03)
ATRCN	(.02, .00, .00)	(.09, .02, .01)	(.16, .01, .00)	(.50, .15, .05)
GLSWW	(.01, .01, .00)	(.10, .01, .00)	(.14, .03, .01)	(.56, .10, .03)

Then, each row of weighted decision matrix is defined as MF-vector. Table 31 shows the weighted decision vectors.

Table 31: Weighted Decision Vectors

Weighted Decision
[(.02, .00, .00), (.09, .02, .00), (.16, .01, .00), (.66, .03, .00)]
[(.02, .00, .00), (.09, .02, .00), (.14, .03, .01), (.56, .10, .03)]
[(.02, .00, .00), (.10, .01, .00), (.14, .03, .01), (.56, .10, .03)]
[(.02, .00, .00), (.09, .02, .01), (.16, .01, .00), (.50, .15, .05)]
[(.01, .01, .00), (.10, .01, .00), (.14, .03, .01), (.56, .10, .03)]

Table 32 gives information about dot products.

Table 32: Dot Products of Weighted Decision Vectors

	ϕ_1	ϕ_2	ϕ_3	ϕ_4	ϕ_5
ϕ_1		.404	.405	.372	.405
ϕ_2	.404		.352	.328	.352
ϕ_3	.405	.352		.329	.354
ϕ_4	.372	.328	.329		.329
ϕ_5	.405	.352	.354	.329	

After that, the cosines of weighted angles are estimated and illustrated in Table 33.

Table 33: Cosines of weighted angles

	$\mathbf{Cos}\,(\mathfrak{Z}_{\phi_1})$	$\mathbf{Cos}\,(\mathfrak{Z}_{\phi_2})$	$\mathbf{Cos}\,(\mathfrak{Z}_{\phi_3})$	$\mathbf{Cos}\,(\mathfrak{Z}_{\phi_4})$	$\mathbf{Cos}\,(\mathfrak{Z}_{\phi_5})$
$Cos\,(\mathfrak{Z}_{\phi_1})$		.989	.988	.970	.988

	$\mathbf{Cos}\,(\mathfrak{Z}_{\phi_1})$	$\mathbf{Cos}\,(\mathfrak{Z}_{\phi_2})$	$\mathbf{Cos}\,(\mathfrak{Z}_{\phi_3})$	$\mathbf{Cos}\,(\mathfrak{Z}_{\phi_4})$	$\mathbf{Cos}\,(\mathfrak{Z}_{\phi_5})$
$Cos\,(\mathfrak{Z}_{\phi_2})$	.989		.999	.993	.999
$Cos\,(\mathfrak{Z}_{\phi_3})$	.988	.999		.992	1.000
$Cos\,(\mathfrak{Z}_{\phi_4})$	.970	.993	.992		.992
$Cos\,(\mathfrak{Z}_{\phi_5})$	.988	.999	1.000	.992	

Later, the weighted decision angle between each pair of MF-vectors is computed using Equation (51). The weighted decision angles are shared in Table 34.

Table 34: Weighted Decision Angles

	$\Im_{\phi_1}$	$\Im_{\phi_2}$	$\Im_{\phi_3}$	$\Im_{\phi_4}$	$\Im_{\phi_5}$
$\Im_{\phi_1}$		.146	.153	.246	.153
$\Im_{\phi_2}$	.146		.033	.121	.036
$\Im_{\phi_3}$	.153	.033		.124	.011
$\Im_{\phi_4}$	.246	.121	.124		.124
$\Im_{\phi_5}$	.153	.036	.011	.124	

Then, the normalized weighted decision angles are obtained regarding to molecular geometry shapes using Equations (52) – (57). The normalized weighted decision angles are summarized in Table 35.

Table 35: Normalized Weighted Decision Angles

Linear	$\backslash\Im_{\phi_1}$	$\backslash\Im_{\phi_2}$	$\backslash\Im_{\phi_3}$	$\backslash\Im_{\phi_4}$	$\backslash\Im_{\phi_5}$
$\backslash\Im_{\phi_1}$	.000	.047	.049	.078	.049
$\backslash\Im_{\phi_2}$	.047	.000	.011	.038	.011
$\backslash\Im_{\phi_3}$	.049	.011	.000	.039	.004
$\backslash\Im_{\phi_4}$	.078	.038	.039	.000	.039
$\backslash\Im_{\phi_5}$	.049	.011	.004	.039	.000
Trigonal Planar	$\backslash\Im_{\phi_1}$	$\backslash\Im_{\phi_2}$	$\backslash\Im_{\phi_3}$	$\backslash\Im_{\phi_4}$	$\backslash\Im_{\phi_5}$
$\backslash\Im_{\phi_1}$	.000	.070	.073	.117	.073
$\backslash\Im_{\phi_2}$	.070	.000	.016	.058	.017
$\backslash\Im_{\phi_3}$	.073	.016	.000	.059	.005
$\backslash\Im_{\phi_4}$	.117	.058	.059	.000	.059
$\backslash\Im_{\phi_5}$	.073	.017	.005	.059	.000
Tetrahedral	$\backslash\Im_{\phi_1}$	$\backslash\Im_{\phi_2}$	$\backslash\Im_{\phi_3}$	$\backslash\Im_{\phi_4}$	$\backslash\Im_{\phi_5}$
$\backslash\Im_{\phi_1}$	.000	.077	.080	.129	.080
$\backslash\Im_{\phi_2}$	.077	.000	.017	.063	.019
$\backslash\Im_{\phi_3}$	.080	.017	.000	.065	.006
$\backslash\Im_{\phi_4}$	.129	.063	.065	.000	.065
$\backslash\Im_{\phi_5}$	.080	.019	.006	.065	.000
Trigonal Bipyramidal	$\backslash\Im_{\phi_1}$	$\backslash\Im_{\phi_2}$	$\backslash\Im_{\phi_3}$	$\backslash\Im_{\phi_4}$	$\backslash\Im_{\phi_5}$
$\backslash\Im_{\phi_1}$	.000	.080	.084	.134	.084
$\backslash\Im_{\phi_2}$	.080	.000	.018	.066	.020
$\backslash\Im_{\phi_3}$	.084	.018	.000	.068	.006
$\backslash\Im_{\phi_4}$	.134	.066	.068	.000	.068
$\backslash\Im_{\phi_5}$	.084	.020	.006	.068	.000
Octahedral	$\backslash\Im_{\phi_1}$	$\backslash\Im_{\phi_2}$	$\backslash\Im_{\phi_3}$	$\backslash\Im_{\phi_4}$	$\backslash\Im_{\phi_5}$
$\backslash\Im_{\phi_1}$	.000	.093	.097	.157	.098
$\backslash\Im_{\phi_2}$	.093	.000	.021	.077	.023
$\backslash\Im_{\phi_3}$	.097	.021	.000	.079	.007
$\backslash\Im_{\phi_4}$	.157	.077	.079	.000	.079
$\backslash\Im_{\phi_5}$	.098	.023	.007	.079	.000

Afterwards, the reciprocal items are estimated by computing the inverse of these normalized weighted decision angles according to multiplication. Table 36 is reciprocal items of decision matrix for linear.

Table 36: Reciprocal Items of Decision (Linear)

	$\mathfrak{r3}_{\phi_1}$	$\mathfrak{r3}_{\phi_2}$	$\mathfrak{r3}_{\phi_3}$	$\mathfrak{r3}_{\phi_4}$	$\mathfrak{r3}_{\phi_5}$
$r\mathfrak{3}_{\phi_1}$		21.473	2.544	12.772	2.502
$r\mathfrak{3}_{\phi_2}$	21.473		94.017	25.985	87.407
$r\mathfrak{3}_{\phi_3}$	2.544	94.017		25.395	285.245
$r\mathfrak{3}_{\phi_4}$	12.772	25.985	25.395		25.352
$r\mathfrak{3}_{\phi_5}$	2.502	87.407	285.245	25.352	

Later, these items are normalized, and a final decision matrix is generated that accepts these normalized items as elements. The final decision matrix for linear is displayed in Table 37.

Table 37: Final Decision Matrix (Linear)

	SWNDW	**TRANS**	**BUSSH**	**ATRCN**	**GLSWW**
SWNDW		.035	.033	.021	.033
TRANS	.035		.152	.042	.141
BUSSH	.033	.152		.041	.461
ATRCN	.021	.042	.041		.041
GLSWW	.033	.141	.461	.041	

Equations (64) – (69) are used for ranking alternative investment policies. The velocity, personal and global best positions are exhibited in Table 38.

Table 38: Velocity, Personal and Global Best Positions

	SWN DW (($\mathbb{V}_1$)(1)	TRA NS (($\mathbb{V}_2$)(	BUS SH (($\mathbb{V}_3$)(1)	ATR CN (($\mathbb{V}_4$)(1)	GLS WW (($\mathbb{V}_5$)(1)	SWN DW ((P_1)(1)	TRA NS ((P_2)(	BUS SH ((P_3)(1)	ATR CN ((P_4)(1)	GLS WW ((P_5)(1)	$((P_{gb})($	$((P_{gb})($ $-((P_{gb}$ $-1))$
SWN DW		.000	.002	.009	.000	.000	.035	.036	.030	.033	.03	-
TRA NS	.078		-.005	.070	.004	.113	.000	.152	.112	.145	.15	-
BUS SH	.285	.209		.276	.012	.318	.361	.000	.317	.473	.46	-
ATR CN	.013	.000	.000		.002	.034	.042	.041	.000	.043	.04	-
GLS WW	.312	.206	.005	.274		.345	.347	.466	.315	.000	.46	-
	SWN DW (($\mathbb{V}_1$)(2)	TRA NS (($\mathbb{V}_2$)(	BUS SH (($\mathbb{V}_3$)(2)	ATR CN (($\mathbb{V}_4$)(2)	GLS WW ((V_5)(2)	SWN DW ((P_1)(2)	TRA NS ((P_2)(	BUS SH ((P_3)(2)	ATR CN ((P_4)(2)	GLS WW ((P_5)(2)	$((P_{gb})($	$((P_{gb})($ $-((P_{gb}$ $-1))$
SWN DW		.00	.00	-.01	.00	.00	.04	.03	.03	.03	.04	.001
TRA NS	-.05		.00	-.05	-.01	.15	.00	.15	.15	.16	.16	.004
BUS SH	-.19	-.16		-.21	.00	.45	.46	.00	.46	.46	.46	.003
ATR CN	-.01	.00	.00		.00	.04	.04	.04	.00	.04	.04	.000
GLS WW	-.15	-.15	-.01	-.19		.42	.46	.46	.45	.00	.46	.001
	SWN DW (($\mathbb{V}_1$)(3)	TRA NS (($\mathbb{V}_2$)(	BUS SH (($\mathbb{V}_3$)(3)	ATR CN (($\mathbb{V}_4$)(3)	GLS WW (($\mathbb{V}_5$)(3)	SWN DW ((P_1)(3)	TRA NS ((P_2)(	BUS SH ((P_3)(3)	ATR CN ((P_4)(3)	GLS WW ((P_5)(3)	$((P_{gb})($	$((P_{gb})($ $-((P_{gb}$ $-1))$
SWN DW		.00	.00	-.01	.00	.00	.04	.03	.03	.04	.04	.000
TRA NS	-.13		.00	-.12	-.02	.15	.00	.16	.15	.16	.16	.000
BUS SH	-.48	-.38		-.49	.00	.45	.46	.00	.46	.46	.46	.000
ATR CN	-.02	.00	.00		.00	.04	.04	.04	.00	.04	.04	.000
GLS WW	-.40	-.39	.00	-.48		.42	.46	.46	.45	.00	.46	.000

At the third iteration, the differences of global best positions are less than the threshold as .001. The average of positions of the alternative investment policies are obtained as .2128, .2008, .1390, .2185, and .1398 respectively. So, the ranking results are given in descending order as ATRCN, SWNDW, TRANS, GLSWW, BUSSH. For consistency and validity of the results, analyses are performed again with all MGS and learning rates. The comparison of the rankings of the alternative investment policies is illustrated in Table 39.

Table 39: Comparison of Rankings of Alternative Investment Policies

$lr = .1$	**Linear**	**Trigonal Planar**	**Tetrahedral**	**Trigonal Bipyramidal**	**Octahedral**
SWNDW	2	2	2	2	2
TRANS	3	3	3	3	3
BUSSH	5	5	5	5	5
ATRCN	1	1	1	1	1
GLSWW	4	4	4	4	4
$lr = .5$	**Linear**	**Trigonal Planar**	**Tetrahedral**	**Trigonal Bipyramidal**	**Octahedral**
SWNDW	2	2	2	2	2
TRANS	3	3	3	3	3
BUSSH	5	5	5	5	5
ATRCN	1	1	1	1	1
GLSWW	4	4	4	4	4
$lr =1$	**Linear**	**Trigonal Planar**	**Tetrahedral**	**Trigonal Bipyramidal**	**Octahedral**
SWNDW	2		2	2	2
TRANS	3	3	3	3	3
BUSSH	5	5	5	5	5
ATRCN	1	1	1	1	1
GLSWW	4	4	4	4	4

When the orders in Table 31 are examined, it is seen that the results are consistent and valid. In the other words, the optimal alternative investment policy for transparent solar panel installations is solar atriums and canopies.

5 Discussion

Regional solar irradiation (radiated power / unit area) is very important for transparent solar panel installation investments. It is directly related to the regions where the panels are installed. Energy efficiency can be longer with the savings obtained from more energy production thanks to the efficiency of solar panels. For example, the findings of a study conducted for Brazil highlight that the most economically viable option for residential buildings would be to use Electric Shower Heads (ESH) in combination with photovoltaic generation systems (Pinto et al., 2025). Integrating photovoltaic (PV) systems into power grids is also becoming increasingly important in Arab countries rich in solar energy. Since solar energy is a critical component of sustainable development, it has the potential to advance energy systems in politically and economically sensitive countries such as Palestine and Jordan (Ayasi et al., 2025). These countries are sun-rich countries. In this context, if the solar irradiation is high in the installation of transparent solar panels, the efficiency of the installations is generally expected to increase. This indicates the impact of regional climate conditions on long-term sustainability. This also depends on the regional solar irradiation. According to Abdoos et al. (2025), significant growth in solar energy production could occur by 2050 for countries such as Egypt, Turkey, Spain, France, and Greece. At this point, technological advancements and supportive policies are crucial. Energy production efficiency is not independent of local climatic conditions. Therefore, regional solar irradiance is an important criterion for issues such as long-term sustainability and installation costs (Zhang et al., 2024; Xuan et al., 2024). In this context, the effect of the relationship between ambient temperature and solar irradiation is important for research. The best energy gain is observed in temperate climate regions where extreme cold conditions are not present (Ozturk et al., 2024; Miranda-Jiménez et al., 2024).

ROI, which shows how profitable the investment is, is also used to evaluate whether transparent solar panels are profitable. In this context, competitive payback periods and positive returns on investment are essential for residential PV systems to provide cost-effective energy solutions (Shand et al., 2025). When optimum PV system configurations are achieved, carbon emissions and costs must also be balanced. In this context, solar irradiation has a significant impact on the economy (Zhao et al., 2025; Luo et al., 2024). As stated by Sierro and Blumer (2025), investment in PV

systems excludes low-income groups, homeowners with unsuitable roofs, and tenants. To expand this, citizen-financed photovoltaic (CiFi PV) projects can offer an effective solution. Additionally, the limited availability of land for renewable energy installations makes rooftop solar photovoltaic systems particularly advantageous. Therefore, decreasing prices of PV systems significantly enhance the economic appeal of investing in solar energy. The findings suggest that PV systems can provide effective protection against inflation in regions where they are applicable (Sadat et al., 2025). Furthermore, as inflation increases and taxes are factored in, the returns on these investments become more attractive. The changing ratios of ROI and internal rate of return (IRR) also highlight the role of regional financial factors and inflation in the evaluation of PV systems (Tro-Cabrera et al., 2025; Sadat and Pearce, 2025).

6 Conclusion

This study is conducted to determine the most critical factors affecting the performance of transparent solar panel investments. To achieve this goal, an integrated molecular fuzzy decision-making model is proposed. In the developed model, expert weights are dynamically determined by the q-learning algorithm. Criteria weights are calculated by the LSO method. Alternative investment strategies are ranked by MOPSO. In addition, molecular fuzzy sets are used to manage uncertainties more effectively. The results indicate that the criterion that affects the performance most in transparent solar panel investments is the regional solar radiation level. In addition, solar atriums and awnings and solar-powered smart glass window systems stand out as the most effective investment strategies. These results offer concrete suggestions that will enable businesses to increase their performance by using their resources more efficiently. This study contributes to the literature by proposing an innovative molecular fuzzy decision-making model that manages uncertainties more effectively to select the most appropriate investment strategies for transparent solar panel investments.

There are also some limitations to this study. The results of this model depend on a limited number of expert opinions. The limited number of experts may reduce generalizability, especially for different geographical regions or market conditions. In future studies, the opinions of more experts from more diverse fields can be sought. The generalizability of the model can be increased with this application. In addition, the criteria used are limited to technological, environmental and economic factors. Some important factors such as the effectiveness of legal regulations can also affect this process. A more comprehensive set of criteria can be taken into consideration in future studies. Another limitation is that the model focuses only on the evaluation of current investment strategies. On the other hand, issues such as trade wars and pandemics that affect the economic performance of many countries in the world may also occur. In this context, in the following studies, scenario analyses based on these radical changes can be performed.

Acknowledgement

This research is partially supported by the science and technology innovation Program of Hunan Province #2024RC4008 and AC2024040911247631ff26.

References

[1] M. Abdoos, H. Rashidi, P. Esmaeili, H. Yousefi, M. H. Jahangir, *Forecasting solar energy generation in the Mediterranean region up to 2030–2050 using convolutional neural networks (CNN)*, Cleaner Energy Systems, **10** (2025), 100167. https://doi.org/10.1016/j.cles.2024.100167

[2] J. Abu Qadourah, S. Alnusairat, *Integrating aesthetics and sustainability: Evaluating the aesthetic perception of photovoltaic installation on the apartment building façade in Jordan*, Archnet-IJAR, 2025. https://doi.org/10.1108/ARCH-02-2024-0038

[3] B. A. Akgul, M. S. Ozyazici, M. F. Hasoglu, *Estimation of optimal tilt angles and solar radiation collected by fixed and tracking solar panels for the Mediterranean region*, Turkey Indian Journal of Physics, **98** (2024), 1187-1200. https://doi.org/10.1007/s12648-023-02894-7

[4] M. Almadhhachi, I. Seres, I. Farkas, *Harnessing solar power with aesthetic innovation: An in-depth study on spherical and hemispherical photovoltaic configurations*, Energy Science and Engineering, **12**(5) (2024), 1888-1901. https://doi.org/10.1002/ese3.1717

[5] A. S. Andrade-Arias, G. Kabir, M. Mirmohammadsadeghi, A. Gunasekaran, A. Elizondo-Noriega, *Exploring public perspectives on solar energy adoption in Mexico*, Renewable and Sustainable Energy Reviews, **212** (2025), 115410. https://doi.org/10.1016/j.rser.2025.115410

[6] E. Aramendia, P. E. Brockway, P. G. Taylor, et al., *Estimation of useful-stage energy returns on investment for fossil fuels and implications for renewable energy systems*, Natural Energy, **9** (2024), 803-816. https://doi.org/10.1038/s41560-024-01518-6

[7] B. Ayasi, I. X. Vázquez, M. Saleh, et al., *Application of spiking neural networks and traditional artificial neural networks for solar radiation forecasting in photovoltaic systems in Arab countries*, Neural Computing and Applic, (2025). https://doi.org/10.1007/s00521-025-11066-z

[8] S. Aziz, S. A. Chowdhury, M. Alauddin, *Investment risks and policy solutions for renewable electricity in Bangladesh*, Energy for Sustainable Development, **85** (2025), 101605. https://doi.org/10.1016/j.esd.2024.101605

[9] P. Bonomo, F. Frontini, *Building integrated photovoltaics (BIPV): Analysis of the technological transfer process and innovation dynamics in the Swiss building sector*, Buildings, **14**(6) (2024), 1510. https://doi.org/10.3390/buildings14061510

[10] P. Bonomo, F. Frontini, R. Loonen, A. H. M. E. Reinders, *Comprehensive review and state of play in the use of photovoltaics in buildings*, Energy and Buildings, **323** (2024), 114737. https://doi.org/10.1016/j.enbuild.2024.114737

[11] A. Borja Block, J. Escarre Palou, M. Courtant, A. Virtuani, G. Cattaneo, M. Roten, H. Y. Li, M. Despeisse, A. Hessler-Wyser, U. Desai, et al., *Colouring solutions for building integrated photovoltaic modules: A review*, Energy and Building, **314** (2024), 114253. https://doi.org/10.1016/j.enbuild.2024.114253

[12] S. Budhiraja, S. Agrawal, N. Sharma, *Infrared and visible image fusion based on sparse representation and weighted least square optimization*, IETE Journal of Research, (2025), 1-13. https://doi.org/10.1080/03772063.2025.2469642

[13] L. Chen, J. Wang, Z. Wu, Y. Yu, M. Zhou, G. Li, *5G and energy internet planning for power and communication network expansion*, Iscience, **27**(3) (2024). https://doi.org/10.1016/j.isci.2024.109290

[14] H. Dinçer, S. Yüksel, G. O. Olaru, S. Eti, *Integrated information system based on Q-learning algorithm and multi-objective particle swarm optimization with molecular fuzzy-based decision-making for corporate environmental investments*, Information Sciences, **698** (2025), 121757. https://doi.org/10.1016/j.ins.2024.121757

[15] N. Fahoum, M. Sitbon, *Effects of building color, material, and angle on bifacial and transparent solar panels*, Processes, **13**(2) (2025), 480. https://doi.org/10.3390/pr13020480

[16] S. Forhad, M. S. Hossen, S. Noman, I. A. Diba, F. Mahmud, M. O. Ullah, M. R. K. Shuvo, *Influence of a dual axis IoT-based off-grid solar tracking system and Wheatstone bridge on efficient energy harvesting and management*, Journal of Engineering Research and Reports, **26**(3) (2024), 125-136. https://doi.org/10.9734/jerr/2024/v26i31099

[17] K. Fragkos, G. Charalampous, I. Fountoulakis, K. Papachristopoulou, D. Hadjimitsis, S. Kazadzis, *Next-day solar irradiance forecasting: A preliminary study in Limassol*, 2024 3rd International Conference on Energy Transition in the Mediterranean Area (SyNERGY MED), Limassol, Cyprus, 2024, 1-5, 10.1109/SyNERGYMED62435.2024.10799286

[18] H. Gholami, *A holistic multi-criteria assessment of solar energy utilization on urban surfaces*, Energies, **17**(21) (2024), 5328. https://doi.org/10.3390/en17215328

[19] M. Gholami, A. Arefi, A. Hasan, et al., *Enhancing energy autonomy of greenhouses with semi-transparent photovoltaic systems through a comparative study of battery storage systems*, Scientific Reports, **15** (2024), 2213. https://doi.org/10.1038/s41598-025-85418-z

[20] A. Habchi, B. Hartiti, H. Labrim, P. Thevenin, E. Ntsoenzok, *Amplification of green hydrogen production using an innovative new hybrid semi-transparent photovoltaic solar panel integrated with tubular thermoelectric generators*, Applied Energy, **384** (2025), 125464. https://doi.org/10.1016/j.apenergy.2025.125464

[21] A. Hussain, M. Umair, S. Khan, W. B. Alonazi, S. S. Almutairi, A. Malik, *Exploring sustainable healthcare: Innovations in health economics, social policy, and management*, Heliyon, **10**(13) (2024), e33186. https://doi.org/10.1016/j.heliyon.2024.e33186

[22] H. A. Kazem, M. T. Chaichan, A. H. Al-Waeli, K. Sopian, *Recent advancements in solar photovoltaic tracking systems: An in-depth review of technologies, performance metrics, and future trends*, Solar Energy, **282** (2024), 112946. https://doi.org/10.1016/j.solener.2024.112946

[23] K. Kumba, P. Upender, P. Buduma, M. Sarkar, S. P. Simon, V. Gundu, *Solar tracking systems: Advancements, challenges, and future directions: A review*, Energy Reports, **12** (2024), 3566-3583. https://doi.org/10.1016/j.egyr.2024.09.038

[24] Z. Li, J. Ma, Q. Wang, M. Wang, F. Jiang, *Enhancing urban solar irradiation prediction with shadow-attention graph neural networks: Implications for net-zero energy buildings in New York City*, Sustainable Cities and Society, **120** (2025), 106133. https://doi.org/10.1016/j.scs.2025.106133

[25] T. Liu, M. M. Almutairi, J. Ma, A. Stewart, Z. Xing, M. Liu, Y. Cho, *Solution-processed thin film transparent photovoltaics: Present challenges and future development*, Nano-Micro Letters, **17**(1) (2025), 49. https://doi.org/10.1007/s40820-024-01547-6

[26] H. Luo, M. Vasiliev, T. He, P. Wang, J. Lyford, V. Rosenberg, C. Li, *Transparent solar photovoltaic windows provide a strong potential for self-sustainable food production in forward-looking greenhouse farming architectures*, Cleaner Engineering and Technology, (2025), 100895. https://doi.org/10.1016/j.clet.2025.100895

[27] X. Luo, Y. Zhang, J. Lu, J. Ge, *Multi-objective optimization of the office park building envelope with the goal of nearly zero energy consumption*, Journal of Building Engineering, **84** (2024), 108552. https://doi.org/10.1016/j.jobe.2024.108552

[28] S. Minazhova, M. Kurrat, B. Ongar, A. Georgiev, *Deploying a rooftop PV panels in the southern regions of Kazakhstan*, Energy, (2025), 135205. https://doi.org/10.1016/j.energy.2025.135205

[29] R. Miranda-Jiménez, O. Vigil-Galán, J. R. González-Castillo, A. R. Terán-Cuevas, M. E. Gutiérrez-Castillo, L. R. Tovar-Gálvez, *Solar PV technologies selection for the design of photovoltaic installations in Mexico based on the analysis of meteorological satellite data from the region*, Atmósfera, **38** (2024). https://doi.org/10.20937/atm.53282

[30] Z. Ozturk, M. Terkes, A. Demirci, *Optimal planning of hybrid power systems under economic variables and different climatic regions: A case study of Türkiye*, Renewable Energy, **232** (2024), 121029. https://doi.org/10.1016/j.renene.2024.121029

[31] J. A. Pinto, G. L. Tiago Filho, A. L. C. de Jesus, M. D. G. Barbedo, I. F. S. dos Santos, R. M. Barros, F. D. G. B. da Silva, *A comparative analysis of thermosolar and photovoltaic systems for meeting residential hot water demands*, Renewable Energy, (2025), 122652. https://doi.org/10.1016/j.renene.2025.122652

[32] A. Qamili, S. Kapia, *Evaluation and integration of photovoltaic (PV) systems in Albanian energy landscape*, Solar Compass, **10** (2024), 100070. https://doi.org/10.1016/j.solcom.2024.100070

[33] S. A. Sadat, K. Mittal, J. M. Pearce, *Using investments in solar photovoltaics as inflation hedges*, Energies, **18**(4) (2025), 890. https://doi.org/10.3390/en18040890

[34] S. A. Sadat, J. M. Pearce, *Techno-economic evaluation of electricity pricing structures on photovoltaic and photovoltaic-battery hybrid systems in Canada*, Renewable Energy, **242** (2025), 22456. https://doi.org/10.1016/j.renene.2025.122456

[35] J. Shand, E. Glakpe, C. Ivey, *Policy implications of implementing residential PV solar energy systems in developing regions*, Energy Policy, **196** (2025), 114414. https://doi.org/10.1016/j.enpol.2024.114414

[36] Y. Shen, W. Liu, H. Dinçer, S. Yüksel, *Hybrid molecular fuzzy recommender systems for impact of climate change on renewable energy performance*, Renewable Energy, **245** (2025), 122799. https://doi.org/10.1016/j.renene.2025.122799

[37] F. Sierro, Y. Blumer, *Collective action without community? Perspectives from project developers and participants in citizen-financed photovoltaic projects*, Energy Research and Social Science, **119** (2025), 103856. https://doi.org/10.1016/j.erss.2024.103856

[38] P. N. Tham, T. D. Thuy, P. K. Nam, E. Papyrakis, *Policy uncertainty, public perception, and the preferences for rooftop solar power systems: A choice experiment study in Vietnam*, Renewable and Sustainable Energy Reviews, **208** (2025), 115067. https://doi.org/10.1016/j.rser.2024.115067

[39] A. Tro-Cabrera, R. Lago-Aurrekoetxea, I. Martínez-de-Alegría, E. Villamor, A. Campos-Celador, *A methodology for assessing rooftop solar photovoltaic potential using GIS open-source software and the EROI constraint*, Energy and Buildings, (2025), 115401. https://doi.org/10.1016/j.enbuild.2025.115401

[40] M. Umair, W. Ahmad, B. Hussain, C. Fortea, M. L. Zlati, V. M. Antohi, *Empowering Pakistan's economy: The role of health and education in shaping labor force participation and economic growth*, Economies, **12**(5) (2024), 113. https://doi.org/10.3390/economies12050113

[41] Y. Wang, S. Lee, C. Li, et al., *Techno-economic evaluation of solar photovoltaic power production in China for sustainable development and the environment*, Environ Dev Sustain, (2024). https://doi.org/10.1007/s10668-024-05837-2

[42] H. Wang, X. Wang, Y. Yin, X. Deng, M. Umair, *Evaluation of urban transportation carbon footprint—Artificial intelligence based solution*, Transportation Research Part d: Transport and Environment, **136** (2024), 104406. https://doi.org/10.1016/j.trd.2024.104406

[43] Z. Wu, Z. Chen, C. Wang, M. Zhou, J. Wang, L. Chen, *Unlocking the potential of rooftop solar panels: An incentive rate structure design*, Energy Policy, **190** (2024), 114159. https://doi.org/10.1016/j.enpol.2024.114159

[44] Q. Xuan, N. Yang, M. Kai, C. Wang, B. Jiang, X. Liu, B. Zhao, *Combined daytime radiative cooling and solar photovoltaic/thermal hybrid system for year-round energy saving in buildings*, Energy, **304** (2024), 132178. https://doi.org/10.1016/j.energy.2024.132178

[45] Y. Zhang, *Enhancing solar irradiance prediction for sustainable energy solutions employing a hybrid machine learning model; improving hydrogen production through Photoelectrochemical device*, Applied Energy, **382** (2025), 125280. https://doi.org/10.1016/j.apenergy.2025.125280

[46] H. Zhang, X. Chen, W. Li, R. Peng, J. Ji, X. Su, C. Luo, *Energy, economic, emissions analysis of semi-flexible crystalline silicon photovoltaic system integrated with factory building roofs based on actual electricity load and cost conditions*, Energy and Buildings, **330** (2025), 115358. https://doi.org/10.1016/j.enbuild.2025.115358

[47] T. Zhang, J. Zhai, Z. Shi, Q. Li, J. Cai, *Comparison of PV and PV/T systems in different regions of China: Energy gain, energy cost, energy payback and energy return*, Energy and Built Environment, (2024). https://doi.org/10.1016/j.enbenv.2024.12.001

[48] N. Zhao, J. Zhang, C. Ding, *Integrated 3E impacts of photovoltaic systems: A comparative study of panels and windows*, Case Studies in Thermal Engineering, **66** (2025), 105736. https://doi.org/10.1016/j.csite.2024.105736